

UNIVERSITÀ CATTOLICA DEL SACRO CUORE
SEDE DI BRESCIA

Facoltà di Scienze Matematiche, Fisiche e Naturali

Corso di Laurea in Fisica



Tesi di Laurea Magistrale

Dynamics of the Symmetry Breaking
in Ordered Phases

Relatore:

Ch.mo Prof. Claudio Giannetti

Correlatore:

Ch.mo Prof. Francesco Banfi

Candidato:

Marco Gandolfi

Matricola n. 4108849

Anno Accademico 2013/2014

15 dicembre 2014

Contents

1	Model	12
1.1	The Ginzburg-Landau Theory	12
1.2	Equation for a spatially inhomogeneous time-independent order parameter	17
1.3	Ginzburg-Landau equation for a spatially inhomogeneous time-dependent order parameter	21
1.4	Linearized Ginzburg-Landau equation for a spatially inhomogeneous time-dependent order parameter	23
2	COMSOL Multiphysics main features	25
3	Dynamics of the order parameter in the homogeneous case	29
3.1	Time-independent equilibrium order parameter with no damping	29
3.1.1	Results	29
3.1.2	Technical details	37
3.2	Time-independent equilibrium order parameter with damping	38
3.2.1	Results	38
3.2.2	Technical details	44
3.3	Time-dependent equilibrium order parameter with no damping	45
3.3.1	Results	45
3.3.2	Technical details	49
4	Reflectivity for a system in overdamped regime	50
4.1	Results	54
4.1.1	Homogeneous excitation	54
4.1.2	Quasi-homogeneous excitation	63
4.1.3	Strongly inhomogeneous excitation	67
4.1.4	Bulk system	71
4.1.5	Comparison of the analyzed cases	75
4.1.6	Bulk system: comparison between simulations and experimental data	77

4.2	Technical details	85
5	Super-lattice composed by materials with broken symmetry	91
5.1	Many unit cells geometry	93
5.2	One unit cell geometry	97

Introduction

When a second order phase transition occurs you can introduce an order parameter η , obeying to the well-known Ginzburg-Landau equation.

This equation is very general, because it applies for any second order phase transition. There are a lot of applications, such as the study evolution of the order parameter in superconductors or the analyze of the Higgs modes. There is an important link between the superconductivity and the Higgs mechanism: in both cases there is a symmetry breaking.

In particular, as we will see in chapter 1, the free energy for a superconductor assumes the “Mexican hat” shape, with a degenerate circle of minima (the ground state), defined by the order parameter $\eta = Ae^{i\varphi}$, (see figure 1).

In Quantum Field Theory there is an analogy because the Lagrangian can be written as a function of the field η :

$$L = \partial^\mu \eta \partial_\mu \eta - V(\eta),$$

where the potential $V(\eta)$ has the “Mexican hat” shape:

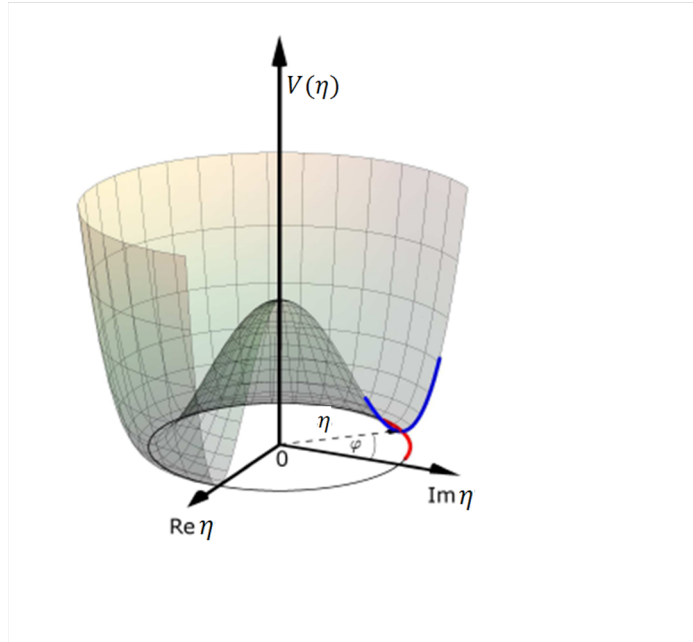


Figure 1: “Mexican hat”: plot of the potential (or of the free energy) V as a function of the field (or of the order parameter) η .

From the ground state there can be two types of excitations:

- Transverse *Nambu-Goldstone* modes (or phase modes), corresponding to the red line in figure 1. They are gapless and massless modes.
- Longitudinal *Higgs* modes (or amplitude modes), corresponding to the blue line in figure 1. In particle physics this modes are massive and manifest as the Higgs boson. They have gap.

It is also important to solve the Ginzburg-Landau equation numerically, because simulations can be useful to predict the behavior of many physical situations, such as the reflectivity of a superconductor.

To measure the reflectivity of a sample, the “Pump and Probe” technique is widespread. With this technique a system in equilibrium is perturbed by a laser pulse (Pump) changing the properties. Using another laser pulse (Probe), we can analyze the reflectivity of the system in the perturbed state.

As time passes the system tends to return in the equilibrium state. With the probe pulse we can analyze the reflectivity variations in time to discover the system properties.

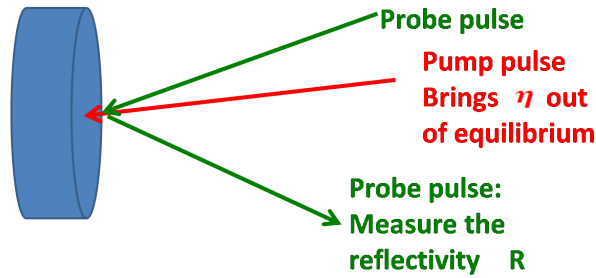


Figure 2: Scheme of the “Pump and Probe” technique.

In this work we introduce the Ginzburg-Landau theory (chapter 1), analyzing the cases of spatially homogeneous and of spatially inhomogeneous time-dependent order parameter.

In the following chapters we try to solve Ginzburg-Landau differential equation numerically, using COMSOL Multiphysics software.

In particular, in chapter 3 we solve this equation for the case of a spatially homogeneous and time dependent order parameter.

In chapter 4 we deal with a spatially inhomogeneous and time dependent order parameter, which is brought out of equilibrium by a laser pulse. We analyze a system in which there is an incoherent propagation of the perturbation, reproducing the diffusion of the energy. At the end of this chapter we compare the simulations with the experimental reflectivity of a superconductor.

In chapter 5 we introduce a super-lattice composed by materials with broken symmetry, satisfying Ginzburg-Landau equation. We analyze the dispersion relation for a wave packet propagating through the super-lattice, and we try to understand if there are frequency gaps. In particular we simulate a super-lattice using a 6-cells geometry and a 1-cell geometry, with periodic boundary conditions.

We report also a brief chapter explaining the main features of COMSOL Multiphysics software (see chapter 2).

In the next chapters we report also some brief sections in which we explain the technical criteria (referring to chapter 2) used to obtain the reported solutions.

References

1. Daniel Sherman, Uwe S. Pracht, Boris Gorshunov, Shachaf Poran, John Jesudasan, Madhavi Chand, Pratap Raychaudhuri, Mason Swanson, Nandini Trivedi, Assa Auerbach, Marc Scheffler, Aviad Frydman, Martin Dressel, *The Higgs Mode in Disordered Superconductors Close to a Quantum Phase Transition*.
2. Ryusuke Matsunaga, Yuki I. Hamada, Kazumasa Makise, Yoshinori Uzawa, Hirotaka Terai, Zhen Wang, Ryo Shimano, *Higgs Amplitude Mode in the BCS Superconductors $Nb_{1-x}Ti_xN$ induced by Terahertz Pulse Excitation*, Physical Review Letters, 2013.
3. Ryusuke Matsunaga, Naoto Tsuji, Hiroyuki Fujita, Arata Sugioka, Kazumasa Makise, Yoshinori Uzawa, Hirotaka Terai, Zhen Wang, Hideo Aoki, Ryo Shimano, *Light-induced collective pseudospin precession resonating with Higgs mode in a superconductor*, Siencexpress.
4. M.-A. Méasson, Y. Gallais, M. Cazayous, B. Clair, P. Rodière, L. Cario, A. Sacuto, *Amplitude ‘Higgs’ mode in $2H - NbSe_2$ Superconductor*.
5. Yafis Barlas, C. M. Varma, *Amplitude or Higgs modes in d-wave superconductors*, PHYSICAL REVIEW (2013).
6. T. Cea and L. Benfatto, *On the nature of the Higgs (amplitude) mode in the coexisting superconducting and charge-density-wave state*, (2014).

Dynamics of the Symmetry Breaking
in Ordered Phases

Chapter 1

Model

In this chapter we introduce the Ginzburg-Landau theory for a second order phase transition.

1.1 The Ginzburg-Landau Theory

A physical system experiences a “*phase transition*” when it changes from one state to another with different properties.

Usually a phase transition occurs when some parameters, such as the temperature, the applied magnetic field, the concentration of charge carriers, the pressure, ... , change and cross a critical value. Phase transitions can be classified in:

- *First order phase transitions*, characterized by the following features:
 - The energy¹ of the system has a discontinuity at the critical point.
 - Spatial coexistence of different phases at the critical point.
 - Hysteresis.

An example of first order phase transition is when a solid melts. In this case the control parameter is the temperature of the system.

¹In this case we mean the internal energy U , satisfying the relation $dU = TdS - PdV + \mu dN$, where T is the temperature, S the entropy, P the pressure, V the volume, μ the chemical potential and N the number of particles of the system.

- *Second order phase transitions*, characterized by the following features:
 - The energy of the system is continuous at the critical point but its first derivative (the specific heat C_V) is not continuous.
 - When the phase transition occurs the system loses symmetry.
 - There is an “order parameter”, which is a scalar or a vector quantity equal to 0 when the system is in the state with higher symmetry, and different from 0 when the system is in the state with lower symmetry.
 - When the system is in the state with lower symmetry and moves toward the critical point, the order parameter tends to go to 0 with continuity. At the critical point the order parameter is 0 and the system is in the state with higher symmetry. So in an homogeneous system there cannot be spatial coexistence of different phases at equilibrium.

Examples of second order phase transitions are the transition from ferromagnetic to paramagnetic materials and the transition from a superconducting state to a normal state. In both these cases the control parameter is the temperature of the system. When the temperature falls under a critical value T_c , the system loses symmetry.

In this work we focus our attention on second order phase transitions only.

As mentioned before, the order parameters can be scalars (real or complex), or vectors. In this work we analyze the case in which the order parameter is a scalar.

In the following we will use the following notation: T for the temperature and P the pressure of the system; η for the order parameter; $\Omega(P, T, \dots)$ for the dimensionless free energy (i.e. the free energy divided by a constant energy), expressed as a function of the pressure, of the temperature or of the other control parameters.

We assume that Ω is a function of η and then we can make an expansion:

$$\Omega(P, T, \eta) = \Omega_0(P, T) + c_1\eta + \alpha_2(P, T) |\eta|^2 + c_3 |\eta|^2 \eta + \frac{1}{2}\beta_4(P, T) |\eta|^4 + \dots \quad (1.1)$$

Since the free energy is a real number, the coefficient α_2 and β_4 are real.

Let's assume to work with a dimensionless order parameter.

If the order parameter is small we can cut this expansion to the 4th power.

Next we assume that the system is invariant for the transformation $\eta \rightarrow -\eta$, i.e. the $+\eta$ or $-\eta$ values must give the same configuration. As a consequence, the expansion of the free energy must contain terms with only even powers of η .

If we suppose that the coefficient β_4 does not depend on the temperature we obtain the following expression:

$$\Omega(P, T, \eta) = \Omega_0(P, T) + \alpha_2(P, T) |\eta|^2 + \frac{1}{2}\beta_4(P) |\eta|^4 \quad (1.2)$$

The equilibrium state is obtained when the free energy is minimum. If $\beta_4 < 0$, the free energy from expression (1.2) would continuously decrease for large values of the order parameter; this is in contrast to the assumption that the expansion can be stopped at the 4th power (which implies a small η). Therefore we assume $\beta_4 > 0$.

Now we can evaluate the minimum of the free energy, using:

$$\frac{\partial \Omega}{\partial \eta^*} = 0.$$

Reminding that $|\eta|^2 = \eta\eta^*$, we obtain:

$$\alpha_2(P, T)\eta + \beta_4(P) |\eta|^2 \eta = 0, \quad (1.3)$$

which gives the following solutions:

$$\eta = 0, \quad (1.4)$$

$$|\eta| = \sqrt{-\frac{\alpha_2}{\beta_4}}. \quad (1.5)$$

If $\alpha_2 > 0$, only solution (1.4) represents the minimum (the other solution is imaginary, therefore it has no physical meaning); if $\alpha_2 < 0$, the solution (1.5) represents the minimum (the other solution represents a local maximum, as we can see from the following graph).

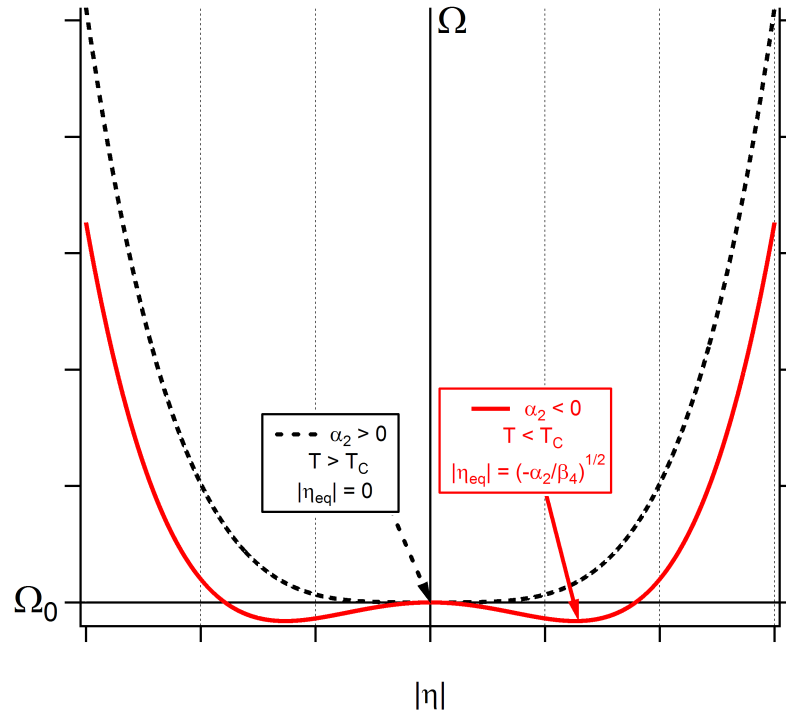


Figure 1.1: Plot of the free energy as a function of the order parameter amplitude. The continuous line describes a case in which $\alpha_2 < 0$; the dashed line describes a case in which $\alpha_2 > 0$.

If $\alpha_2 > 0$ the order parameter at equilibrium is 0, if $\alpha_2 < 0$ the order parameter at equilibrium is $\sqrt{-\alpha_2/\beta_4}$.

As a consequence, it is natural to assume that a phase transition occurs when α_2 changes sign. If the phase transition occurs when the system reaches a critical temperature T_c , we can assume that:

$$\alpha_2(P, T) = a(P) (T - T_c), \quad (1.6)$$

and $a(P)$ is a real positive number. Consequently the order parameter at equilibrium is:

$$|\eta_{eq}| = \begin{cases} 0 & \text{if } T \geq T_c \\ \sqrt{-\frac{a(P)}{\beta_4(P)} (T - T_c)} & \text{if } T < T_c. \end{cases} \quad (1.7)$$

1.2 Equation for a spatially inhomogeneous time-independent order parameter

In this section we deal the case of a spatially inhomogeneous, but time-independent, order parameter analyzing the equilibrium situation.

If the system is characterized by a space-dependent order parameter, the expression of the free energy for a small order parameter becomes:

$$\Omega(P, T, \eta) = \int_V \left[\omega_0(P, T) + A(P, T) |\eta|^2 + \frac{1}{2} B(P) |\eta|^4 + \lambda |\nabla \eta|^2 \right] dV, \quad (1.8)$$

where the last term has been introduced to consider the free energy corrections due to a spatially inhomogeneous order parameter.

The parameter λ is called “stiffness”. If the order parameter is brought out of equilibrium in a certain spatial point, $\sqrt{\lambda}$ describes the spatial scale at which the order parameter has restored to his equilibrium value.

Now we need to calculate the functional derivative of the free energy with respect to η^* . So we make the substitution $\eta \rightarrow \eta + \delta\eta$ to obtain:

$$\begin{aligned} \delta\Omega(P, T, \eta) &= \int_V [\omega_0(P, T) + A(P, T) (\eta + \delta\eta) (\eta^* + \delta\eta^*) + \\ &\quad + \frac{1}{2} B(P) (\eta + \delta\eta)^2 (\eta^* + \delta\eta^*)^2 + \\ &\quad + \lambda \nabla (\eta + \delta\eta) \cdot \nabla (\eta^* + \delta\eta^*)] dV - \Omega(P, T, \eta) = \\ &= \int_V [\omega_0(P, T) + A(P, T) |\eta|^2 + A(P, T) \eta \delta\eta^* + A(P, T) \eta^* \delta\eta \\ &\quad + \frac{1}{2} B(P) |\eta|^4 + B(P) \delta\eta |\eta|^2 \eta^* + B(P) \delta\eta^* |\eta|^2 \eta + O((\delta\eta)^2) + \\ &\quad + \lambda |\nabla \eta|^2 + \lambda \nabla \eta \cdot \nabla \delta\eta^* + \lambda \nabla \eta^* \cdot \nabla \delta\eta + \lambda |\nabla \delta\eta|^2] dV - \Omega(P, T, \eta). \end{aligned}$$

In evaluating the functional derivative of the free energy with respect to η^* we note that:

- All the terms not explicitly containing $\delta\eta^*$ cancel out.

- The terms $O((\delta\eta)^2)$ can be neglected.

$$\frac{\delta\Omega(P, T, \eta)}{\delta\eta^*} = \int_V [A(P, T)\eta + B(P)|\eta|^2\eta] dV + \lambda \frac{\delta}{\delta\eta^*} \int_V [\nabla\eta \cdot \nabla\delta\eta^* + |\nabla\delta\eta|^2] dV.$$

Then we assume that $\nabla\delta\eta$ is small, so we can neglect the last term:

$$\frac{\delta\Omega(P, T, \eta)}{\delta\eta^*} = \int_V [A(P, T)\eta + B(P)|\eta|^2\eta] dV + \lambda \frac{\delta}{\delta\eta^*} \int_V [\nabla\eta \cdot \nabla\delta\eta^*] dV.$$

We evaluate the last integral by parts:

$$\begin{aligned} \frac{\delta\Omega(P, T, \eta)}{\delta\eta^*} &= \int_V [A(P, T)\eta + B(P)|\eta|^2\eta] dV + \lambda \frac{\delta}{\delta\eta^*} (\delta\eta^* \nabla\eta)|_{\partial V} + \\ &\quad - \lambda \frac{\delta}{\delta\eta^*} \int_V [\nabla^2\eta] \delta\eta^* dV. \end{aligned}$$

Finally supposing that on the boundary of the system the order parameter is at equilibrium, so $(\delta\eta^*)|_{\partial V} = 0$, we obtain:

$$\frac{\delta\Omega(P, T, \eta)}{\delta\eta^*} = \int_V [A(P, T)\eta + B(P)|\eta|^2\eta - \lambda\nabla^2\eta] dV. \quad (1.9)$$

The equilibrium solution is when Ω is at a minimum, so from equation (1.9) we obtain:

$$\lambda\nabla^2\eta - A(P, T)\eta - B(P)|\eta|^2\eta = 0. \quad (1.10)$$

Here some examples of equilibrium solutions for a real order parameter:

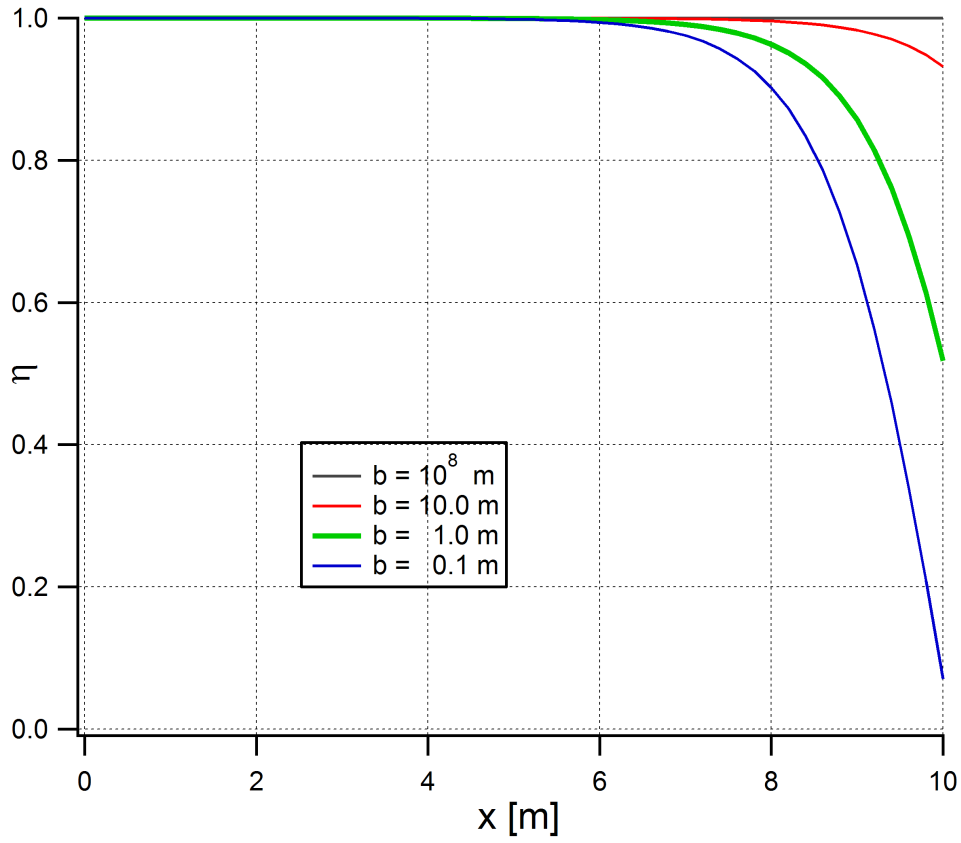


Figure 1.2: Equilibrium solutions for a 1D system (a 10 m line), with $\lambda = 1 \text{ m}^2$, $A = -1$ and $B = 1$. At position $x = 0 \text{ m}$ we apply $\nabla\eta = 0$ boundary condition (bulk system), while at position $x = 10 \text{ m}$ we apply $\nabla\eta = -\eta/b$ boundary condition (interface with another material, characterized by a negligible order parameter). b represents the spatial scale from $x = 10 \text{ m}$ at which the order parameter has fallen to 0). For low b values, the order parameter falls rapidly to 0 (interface with an insulator material); for high b values, the order parameter decreases slowly.

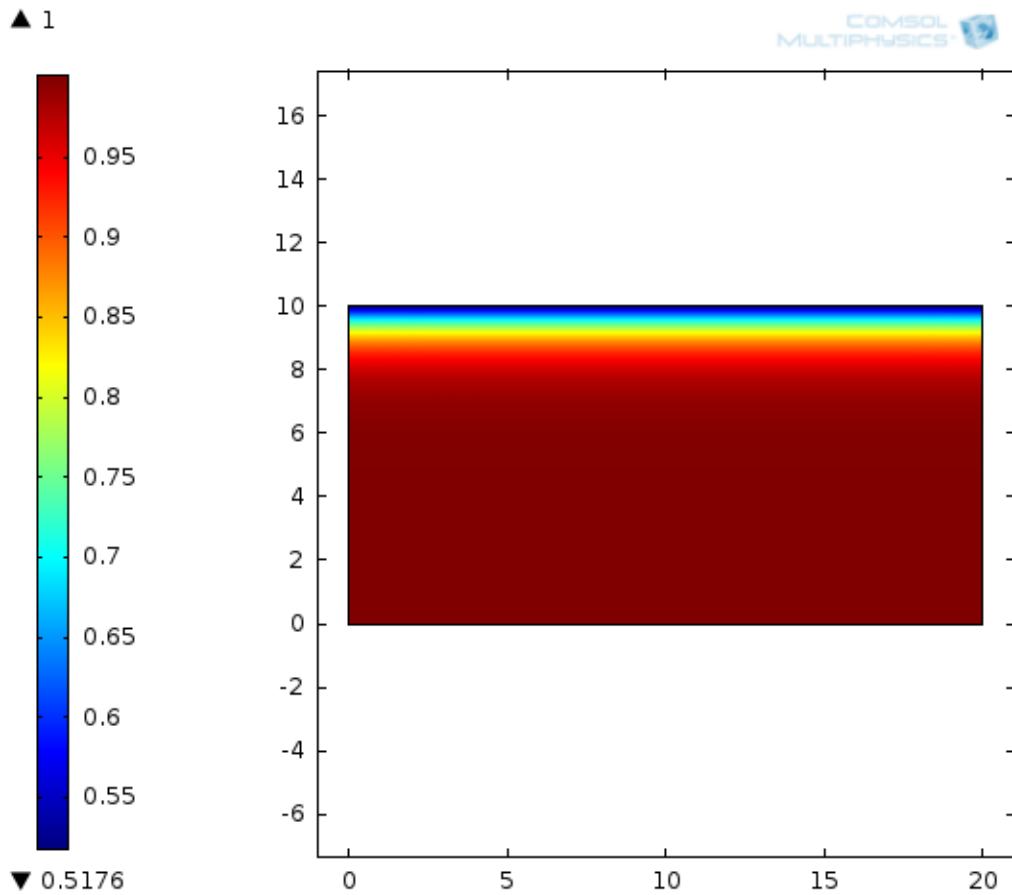


Figure 1.3: Equilibrium solution (color scale) for a 2D system (a 20 m \times 10 m rectangle), with $\lambda = 1 \text{ m}^2$, $A = -1$ and $B = 1$. At vertical sides and lower horizontal side we apply $\nabla\eta = 0$ boundary condition (bulk system), while at upper horizontal side we apply $\nabla\eta = -\eta/b$ boundary condition (interface with another material, characterized by $b = 1 \text{ m}$).

1.3 Ginzburg-Landau equation for a spatially inhomogeneous time-dependent order parameter

In this section we deal the case of a spatially inhomogeneous and time-dependent order parameter.

If η depends also on time and if at a time t_0 it is not at the equilibrium value, the order parameter will move towards the equilibrium value following the motion equation:

$$\frac{\partial^2 \eta}{\partial t^2} + (\alpha\omega) \frac{\partial \eta}{\partial t} = -\omega^2 \frac{\partial \tilde{U}}{\partial \eta^*} = -\omega^2 A(P, T)\eta - \omega^2 B(P) |\eta|^2 \eta + \omega^2 \lambda \nabla^2 \eta. \quad (1.11)$$

This equation is obtained in analogy to the dynamics equation in which $-\partial \tilde{U} / \partial \eta^*$ is the instantaneous force acting on the system (\tilde{U} is the dimensionless free energy per unit volume).

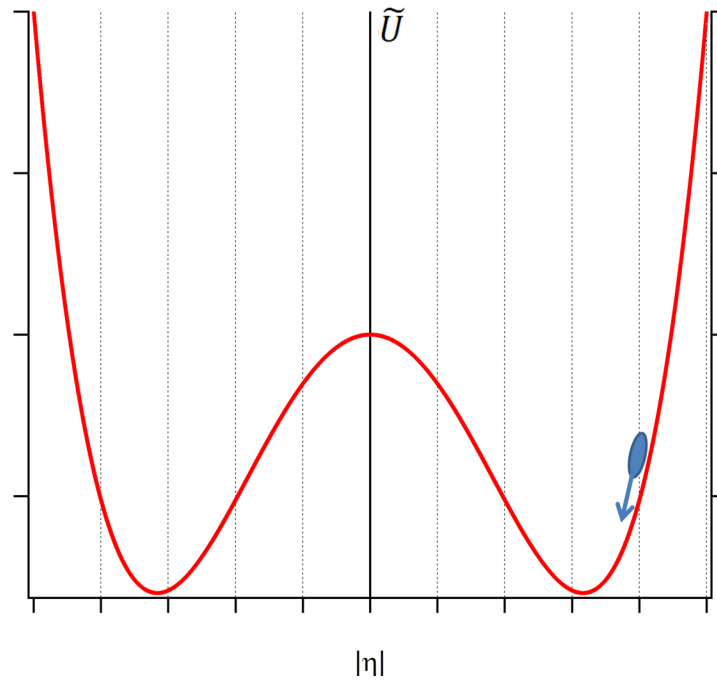


Figure 1.4: Body oscillating in the \tilde{U} potential. Its dynamical equation of motion is analogous to equation (1.11).

In equation (1.11), ω has been introduced to safeguard the dimensions in the equation and is related to the “frequency of oscillation” of η around its equilibrium value.

α is a coefficient representing the “damping” of η .

In the limit $\alpha\omega \gg 1$ relation (1.11) reduces to the original *Ginzburg-Landau Kinetic Equation*:

$$(\alpha\omega) \frac{\partial\eta}{\partial t} = -\omega^2 A(P, T)\eta - \omega^2 B(P) |\eta|^2 \eta + \omega^2 \lambda \nabla^2 \eta, \quad (1.12)$$

describing a system in which the order parameter does not make oscillations. This is a diffusion-like equation, describing an incoherent propagation of the order parameter.

However, since equation (1.11) is more general than equation (1.12), we will deal only with equation (1.11), which is called *Ginzburg-Landau* (GL) equation.

If the order parameter is real, equation (1.11) reduces to:

$$\frac{\partial^2 \eta}{\partial t^2} + (\alpha\omega) \frac{\partial \eta}{\partial t} + \omega^2 A(P, T)\eta + \omega^2 B(P)\eta^3 - \omega^2 \lambda \nabla^2 \eta = 0.$$

This equation has the form of a wave equation in which $\omega^2 A\eta + \omega^2 B\eta^3$ is the source.

Last equation can be rewritten as:

$$\frac{1}{\omega^2} \frac{\partial^2 \eta}{\partial t^2} + \left(\frac{\alpha}{\omega}\right) \frac{\partial \eta}{\partial t} + A(P, T)\eta + B(P)\eta^3 - \lambda \nabla^2 \eta = 0. \quad (1.13)$$

1.4 Linearized Ginzburg-Landau equation for a spatially inhomogeneous time-dependent order parameter

Equation (1.13) contains a cubic term, increasing the difficulties to obtain a solution. Therefore if the order parameter differs from the equilibrium solution slightly we can approximate the cubic term with a linear term in order to obtain a easier to handle equation. In this section we describe the approximation process to linearize equation (1.13).

We suppose that $\eta_{eq}(x)$ is the equilibrium solution of equation (1.13), i.e. $\eta_{eq}(x)$ satisfies relation (1.10) for a real order parameter. Evidently $\eta_{eq}(x)$ does not depend on time.

Defining the displacement of the order parameter with respect to the equilibrium value as:

$$\delta\eta(x, t) = \eta(x, t) - \eta_{eq}(x), \quad (1.14)$$

we can make the substitution $\eta(x, t) \rightarrow \eta_{eq}(x) + \delta\eta(x, t)$ in equation (1.13) to obtain:

$$\begin{aligned} \frac{1}{\omega^2} \frac{\partial^2 \delta\eta}{\partial t^2} + \left(\frac{\alpha}{\omega}\right) \frac{\partial \delta\eta}{\partial t} + A(P, T)\delta\eta + 3B(P)\eta_{eq}^2 \delta\eta + O((\delta\eta)^2) - \lambda \nabla^2 \delta\eta = \\ = \lambda \nabla^2 \eta_{eq} - A(P, T)\eta_{eq} - B(P)\eta_{eq}^3. \end{aligned} \quad (1.15)$$

Reminding that $\eta_{eq}(x)$ satisfies relation (1.10) for a real order parameter, we can deduce that the right-hand side of equation (1.15) is 0.

Further, if the order parameter is slightly different from the equilibrium value, so that the terms $O((\delta\eta)^2)$ can be neglected, we can derive the *Linearized Ginzburg-Landau* equation for a real order parameter:

$$\frac{1}{\omega^2} \frac{\partial^2 \delta\eta}{\partial t^2} + \left(\frac{\alpha}{\omega}\right) \frac{\partial \delta\eta}{\partial t} + [A(P, T) + 3B(P)\eta_{eq}^2] \delta\eta - \lambda \nabla^2 \delta\eta = 0. \quad (1.16)$$

References

1. Michael Tinkham, *Introduction to Superconductivity*, McGraw-Hill, Inc.
2. Anthony James Leggett, *Quantum Liquids. Bose condensation and Cooper pairing in condensed-matter systems*, Oxford Graduate Texts, 2006.

Chapter 2

COMSOL Multiphysics main features

In this chapter we explain briefly the main properties of the used program.

COMSOL Multiphysics is a software for solving differential equations coming from physical problems. Since this work deals with the numerical solutions of the GL equation obtained using the COMSOL Multiphysics software, this brief chapter explains the main features of this program.

As we start the program, a “Model Wizard” procedure allows the user to choose the dimensions of the model:

- “0D”, if the space is not involved in the model.
- “1D”. The spatial coordinate is indicated with x .
- “1D-Axisymmetric”, if the model is in 2 dimensions, but there is a rotational symmetry along the angle φ , so the model involves 1 space variable only, the radial coordinate r .
- “2D”. The spatial coordinates are indicated with (x, y) .
- “2D-Axisymmetric”, if the model is in 3 dimensions, but there is a rotational symmetry along the angle φ , so the model involves 2 space variables only, the radial coordinate r and the height coordinate z .
- “3D”. The spatial coordinates are indicated with (x, y, z) .

Then we will be asked to add a “physics”. Since we need to solve a differential equation, in this work we use:

- “Global ODEs and DAEs” in Chapter 3.
- “Coefficient Form PDE” in all the other Chapters. This type of physics is not available for a “0D” model.

Finally we will be asked to choose the “Study Type”. In particular in this work we use:

- “Stationary Study”, if we are interested in an equilibrium solution, in the case of a time-dependent model.
- “Time Dependent Study”, if we are interested in a solution at different times.
- “Eigenvalue Study”, if we are interested in the eigenvalues of an equation.

Then the “Model Wizard” procedure stops and we can modify the model adding items. To do this we can right-click on each voice in the “Model Builder” space. In particular we can add global “parameters” of the model right-clicking on “Global Definitions”.

We can also use a previous solution as an input function of the model. To do this, under the voice with the name of the model, we can add a interpolation function. If we have not a “0D” model, the voice “Geometry” appears and we can choose the shape of the spatial domains.

Under the voice with the name of the model there is the voice concerning the used physics. In this work we use the following 2 possibilities:

- “Global ODEs and DAEs”, used in Chapter 3, for a “0D” model. Under the voice “Global ODEs and DAEs” there is a voice concerning the equation. The equation is written as:

$$f(u, u_t, u_{tt}) = 0,$$

where u is the solution, while u_t and u_{tt} are the first and the second derivate of u with respect to time.

Here we are allowed to type the expression of $f(u, u_t, u_{tt})$ and the initial values of u_t and u_{tt} .

- “Coefficient Form PDE” in all the other Chapters. This type of physics is not available for a “0D” model. Under the voice “Global ODEs and DAEs” we are asked the dimensions of the dependent variable u and of the “Source term” f in the equation; then there is a voice concerning the equation. The equation is written as:

$$e_a \frac{\partial^2 u}{\partial t^2} + d_a \frac{\partial u}{\partial t} + \nabla \cdot (-c \nabla u - \boldsymbol{\alpha} u + \boldsymbol{\gamma}) + \boldsymbol{\beta} \cdot \nabla u + au = f, \quad (2.1)$$

and we can choose the value of the scalar coefficients e_a , d_a , a , of the vector coefficients $\boldsymbol{\alpha}$, $\boldsymbol{\beta}$, $\boldsymbol{\gamma}$ and of the matrix coefficient c . These coefficients can be a function on the spatial coordinates. As for the source term f , we are asked to introduce a more general expression, which can be a function of the dependent variable u and of space coordinates.

If we choose an “Eigenvalue Study”, COMSOL Multiphysics makes a temporal Fourier transformation on the dependent variable u ; so each derivate with respect to time is substituted by the eigenvalue λ to obtain:

$$\lambda^2 e_a u^2 - \lambda d_a u + \nabla \cdot (-c \nabla u - \boldsymbol{\alpha} u + \boldsymbol{\gamma}) + \boldsymbol{\beta} \cdot \nabla u + a u = f.$$

To solve a “Coefficient Form PDE” it is necessary to assign boundary conditions on all the boundaries of the geometry, holding for all times. In particular we use:

- “Zero Flux” boundary condition:

$$-\mathbf{n} \cdot (-c \nabla u - \boldsymbol{\alpha} u + \boldsymbol{\gamma}) = 0,$$

where \mathbf{n} is the external normal to the boundary.

- “Dirichlet” boundary condition, if the dependent variable is constrained to be a specified value on the boundary.
- “Flux/Source” boundary condition:

$$-\mathbf{n} \cdot (-c \nabla u - \boldsymbol{\alpha} u + \boldsymbol{\gamma}) = g - q u,$$

where \mathbf{n} is the external normal to the boundary.

To solve a “Coefficient Form PDE” it is necessary to assign also the initial value of the dependent variable u (and its first derivative with respect to time) on all the domains. To do this we can type the desired expression under the “Initial Values” voice.

In the case of “Time Dependent Study”, the “Initial Values” expression is the solution at the initial time.

In the case of “Stationary Study” and of “Eigenvalue Study”, the “Initial Values” expression represents an initial guess for the solver. For a well constrained problem, the particular expression assigned as “Initial Values” should not influence the final solution.

COMSOL Multiphysics solves the differential equation using the *Finite Elements Method*. The initial problem to solve is approximated with another problem which has a finite number of unknown parameters.

So the times range and the space domains at which we have to calculate a solution are discretized and the software solves the differential equation at some points only. We can choose the number of discretization points, increasing them to make the solution more precise (but the computational costs increase). Finally, when the software has obtained the solution in all the discretization points, it will make an interpolation to give the solution in all the requested domains and times.

If the model has a geometry (not the 0D), the set of spatial discretization points is called “Mesh”. Acting in “Mesh” voice we can choose the distance and the spatial collocation of the discretization points.

For all the specified physics there is a “Study” node, specifying the algorithms and the parameters used to obtain a solution. In particular for this work, sometimes it is necessary to modify the following voices:

- For a “Stationary Study” it is sometimes necessary to diminish “Relative tolerance” to obtain a more precise solution. Sometimes the number of iteration is not enough to reach a solution satisfying the value of “Relative tolerance”; therefore it could be necessary to increase the “Maximum number of iterations”.
- For a “Time Dependent Study” it is necessary to open the voice “Time-Dependent Solver” under the study node and to choose the “Generalized alpha” Method, instead of the “BDF” Method (which generates numerical errors in the case we are dealing with). Then to improve the precision of the solution we have to set “Manual” at the voice “Steps taken by solver” and than choose an opportune “Time step”. COMSOL Multiphysics solves the differential equation in a discrete number of temporal points. The temporal distance among these points is specified by the “Time step” voice. Once obtained the solution in these points, COMSOL Multiphysics makes an interpolation to give the solution for the times listed under the voice “Step 1: Time Dependent”.
- For an “Eigenvalue Study” we are asked to choose the “Desired number of eigenvalues” and where to search the eigenvalues around. If we choose to search an high number of eigenvalues, we may need to increase the “Maximum number of eigenvalue iterations”, under the voice “Eigenvalue Solver 1”.

Right clicking on “Study” node we can activate a “Parametric Sweep”, i.e. we let vary certain parameters over a specified range and for each value of the parameters the software evaluates a solution.

Chapter 3

Dynamics of the order parameter in the homogeneous case

In this chapter we discuss the solutions of GL equation in the case of a spatially homogeneous order parameter.

In the homogeneous case η does not depend on space coordinates and GL equation reduces to:

$$\frac{1}{\omega^2} \frac{\partial^2 \eta}{\partial t^2} + \left(\frac{\alpha}{\omega}\right) \frac{\partial \eta}{\partial t} + A(P, T)\eta + B(P)\eta^3 = 0. \quad (3.1)$$

In this chapter we try to solve equation (3.1) numerically, using “COMSOL Multiphysics” software, for some values of the parameters ω and α .

3.1 Time-independent equilibrium order parameter with no damping

3.1.1 Results

In the current section we fix the parameters:

- $A \equiv -1$ (dimensionless), in order to obtain a non-zero order parameter;
- $B \equiv 1$ (dimensionless).

From equation (1.10) the equilibrium value is:

$$\eta_{eq} = \sqrt{-\frac{A}{B}} = 1.$$

In this section we fix our attention on the case of a system without damping ($\alpha = 0$).

- For any value of ω and α , if we choose $\eta|_{t=0} = 1$ and $\frac{d\eta}{dt}|_{t=0} = 0 \text{ s}^{-1}$ as initial conditions, the solution is

$$\eta(t) = \eta_{eq} = 1, \quad \forall t > 0$$

since the system is in a stable equilibrium position, so it does not move.

- If we choose $\omega = 10 \text{ s}^{-1}$, $\alpha = 0$ as parameters and $\eta|_{t=0} = 1.1$, $\frac{d\eta}{dt}|_{t=0} = 0 \text{ s}^{-1}$ as initial values, we have the following solution:

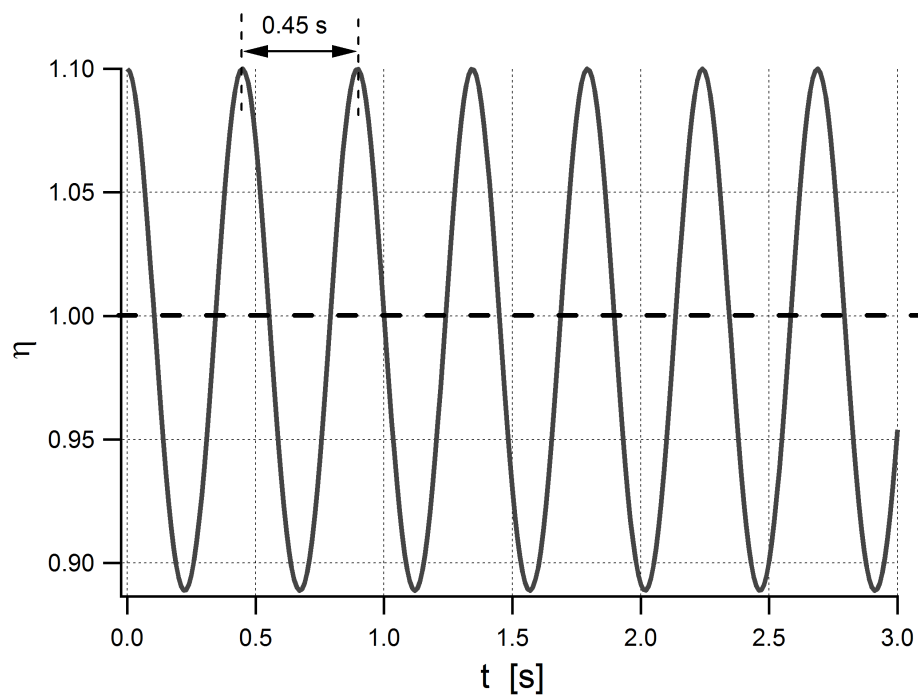


Figure 3.1: Solution for GL equation in the case of homogeneous in space η , with $\omega = 10 \text{ s}^{-1}$, $\alpha = 0$ as parameters and $\eta|_{t=0} = 1.1$, $\frac{d\eta}{dt}|_{t=0} = 0 \text{ s}^{-1}$ as initial values.

The order parameter oscillates around the equilibrium value without symmetry in the amplitude of the oscillation (in opposition to the case of a harmonic oscillator).

The reason of this asymmetry can be found in the shape of the free energy around the minimum. Shown in figure (3.2), the order parameter can go under 0.9 to reach the value that the free energy has at $\eta = 1.1$.

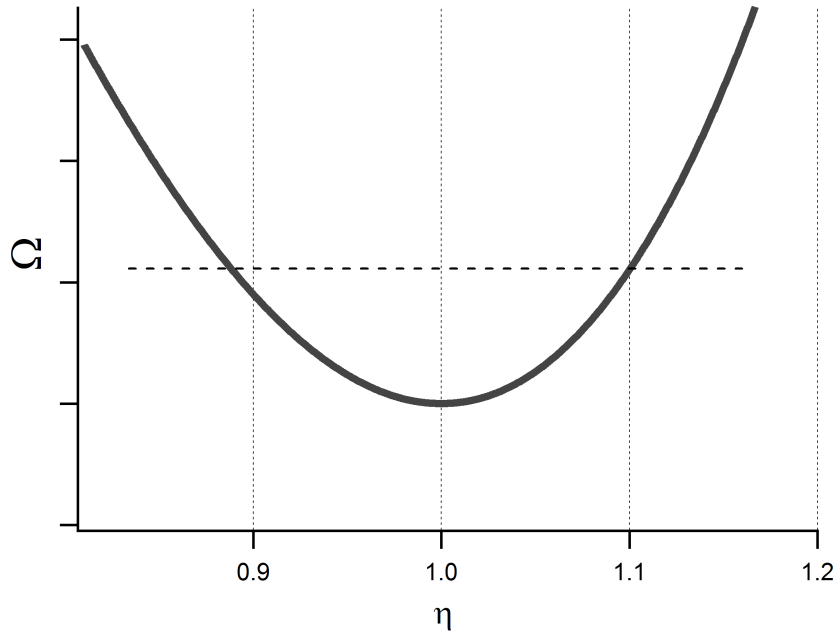


Figure 3.2: The free energy around the equilibrium order parameter, for $A = -1$ and $B = 1$. The dotted line represents the upper limit of the free energy during the oscillation, when initially the order parameter is brought to 1.1.

The period of oscillation is $T = 0.45$ s, which leads to an oscillation frequency:

$$\omega_{osc} = \frac{2\pi}{T} = 13.96 \text{ s}^{-1}.$$

Finally we can note that the amplitude of oscillation does not diminish in time, in accordance with the choice of $\alpha = 0$ (no damping).

Next we make other simulations keeping fixed the parameter $\alpha = 0$ and the initial values $\eta|_{t=0} = 1.1$, $\frac{d\eta}{dt}|_{t=0} = 0 \text{ s}^{-1}$, but changing the parameter ω and we evaluate the frequency of oscillation of the system ω_{osc} . We find the following behavior:

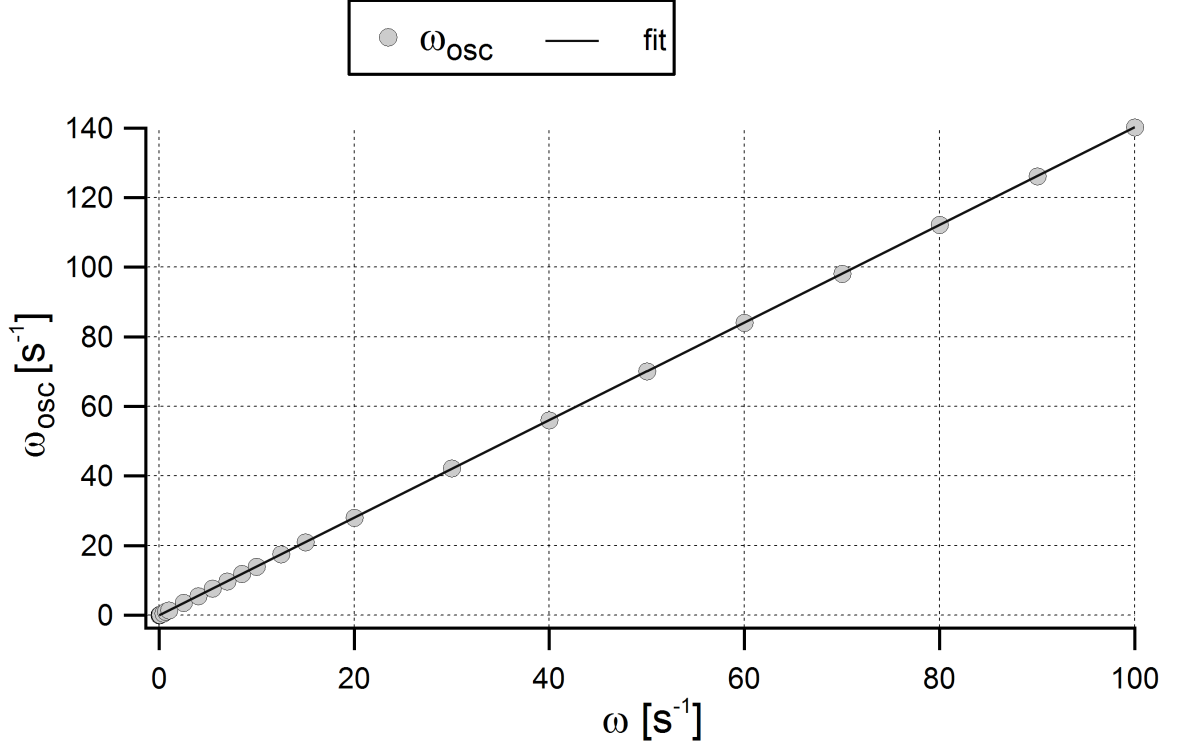


Figure 3.3: Plot of ω_{osc} vs ω (circles) and fit with a line.

Then we fit the data with a line and obtained the following relation:

$$\omega_{osc} = 1.4028 \omega - 0.0350 \text{ s}^{-1}. \quad (3.2)$$

The resulted correlation was 0.999999, therefore the behavior of the oscillation frequency of the system is well reproduced by relation (3.2).

In the reported solutions the displacement of the order parameter $\delta\eta$ with respect to the equilibrium value ($\eta_{eq} = 1$), as defined in equation (1.14), is small.

So in this case equation (3.1) is well approximated by equation (1.16), with $\lambda = 0 \text{ m}^2$:

$$\frac{1}{\omega^2} \frac{\partial^2 \delta\eta}{\partial t^2} + \left(\frac{\alpha}{\omega}\right) \frac{\partial \delta\eta}{\partial t} + [A(P, T) + 3B(P)\eta_{eq}^2] \delta\eta = 0.$$

Inserting the values $A = -1$, $B = 1$, and $\eta_{eq} = 1$, we obtain:

$$\frac{\partial^2 (\delta\eta)}{\partial t^2} + (\alpha\omega) \frac{\partial (\delta\eta)}{\partial t} + \left(\sqrt{2} \omega\right)^2 \delta\eta = 0. \quad (3.3)$$

Finally, imposing $\alpha = 0$ we obtain the equation of an harmonic oscillator with frequency $\omega_{osc} = \sqrt{2} \omega$ (see the appendix), which justifies relation (3.2).

Now we analyze the case in which the order parameter is at equilibrium, but it has a “positive velocity” that brings η out of equilibrium. So we choose $\omega = 10 \text{ s}^{-1}$, $\alpha = 0$ as parameters and $\eta|_{t=0} = 1$, $\frac{d\eta}{dt}|_{t=0} = 1 \text{ s}^{-1}$ as initial values, to obtain the following solution:

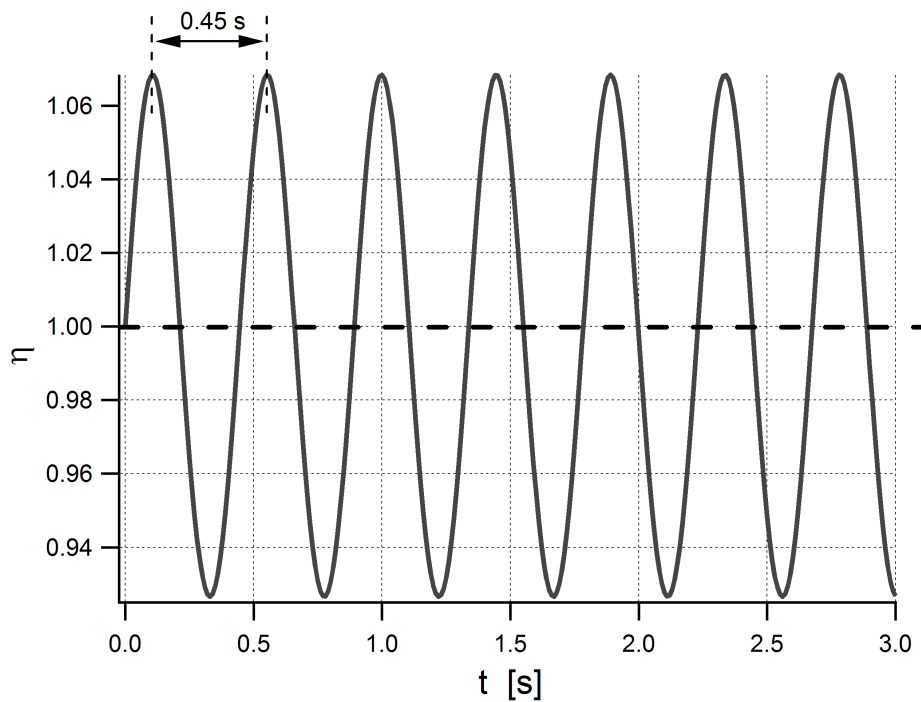


Figure 3.4: Solution for GL equation in the case of homogeneous in space η , with $\omega = 10 \text{ s}^{-1}$, $\alpha = 0$ as parameters and $\eta|_{t=0} = 1$, $\frac{d\eta}{dt}|_{t=0} = 1 \text{ s}^{-1}$ as initial values.

As we can see, all the other conclusions of the previous cases are confirmed here.

Now we treat the effects of nonlinearity on the evolution of the order parameter.

- If we choose $\omega = 10 \text{ s}^{-1}$, $\alpha = 0$ as parameters and $\eta|_{t=0} = 0.1$, $\frac{d\eta}{dt}|_{t=0} = 0 \text{ s}^{-1}$ as initial values, we have the following solution:

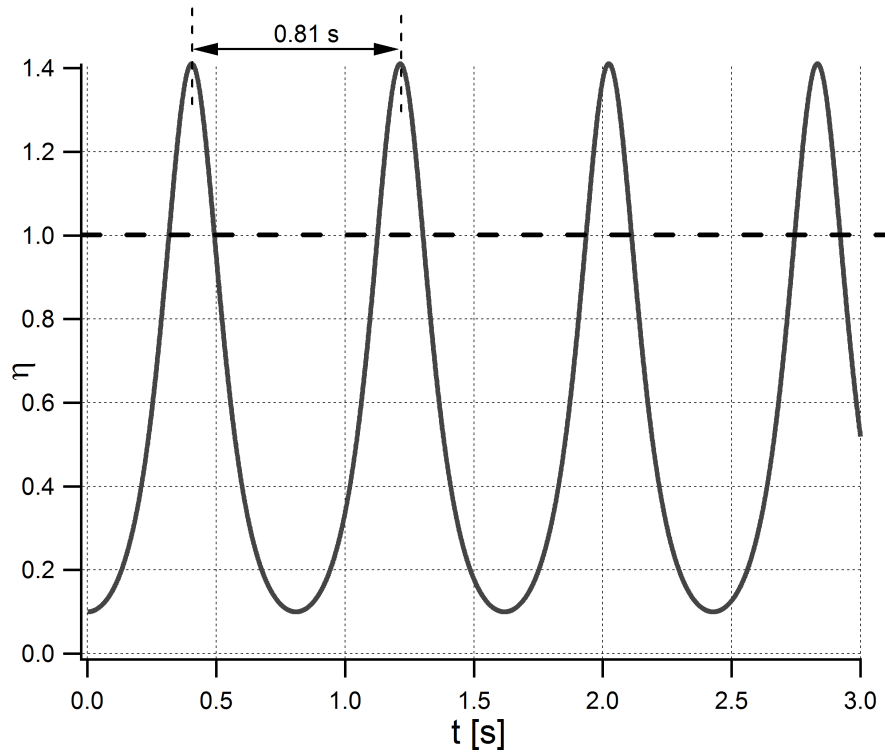


Figure 3.5: Solution for GL equation in the case of homogeneous in space η , with $\omega = 10 \text{ s}^{-1}$, $\alpha = 0$ as parameters and $\eta|_{t=0} = 0.1$, $\frac{d\eta}{dt}|_{t=0} = 0 \text{ s}^{-1}$ as initial values.

The asymmetry of the amplitude of the order parameter oscillation increases, as you can see from the behavior of the free energy:

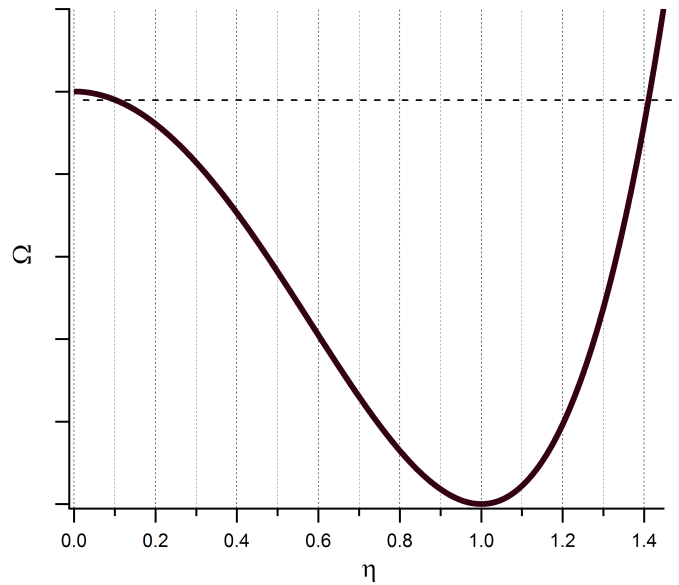


Figure 3.6: The free energy, for $A = -1$ and $B = 1$. The dotted line represents the upper limit of the free energy during the oscillation, when initially the order parameter is brought to 0.1.

As you can see from figure 3.5, the system “spends” less time around $\eta = 1.4$ with respect to $\eta = 0.1$. This can be justified watching figure 3.6: actually Ω has a greater slope around $\eta = 1.4$ than around $\eta = 0.1$, so the force moving the order parameter towards the equilibrium is greater around $\eta = 1.4$ and therefore the order parameter leaves $\eta = 1.4$ more quickly.

The period of oscillation is $T = 0.81$ s, which leads to an oscillation frequency:

$$\omega_{osc} = \frac{2\pi}{T} = 7.757 \text{ s}^{-1}.$$

We can note that the amplitude of oscillation does not diminish in time, in accordance with the choice of $\alpha = 0$ (no damping).

Next we make other simulations keeping fixed the parameter $\alpha = 0$ and the initial values $\eta|_{t=0} = 0.1$, $\frac{d\eta}{dt}|_{t=0} = 0 \text{ s}^{-1}$, but changing the parameter ω and we evaluate the frequency of oscillation of the system ω_{osc} . We find the following behavior:

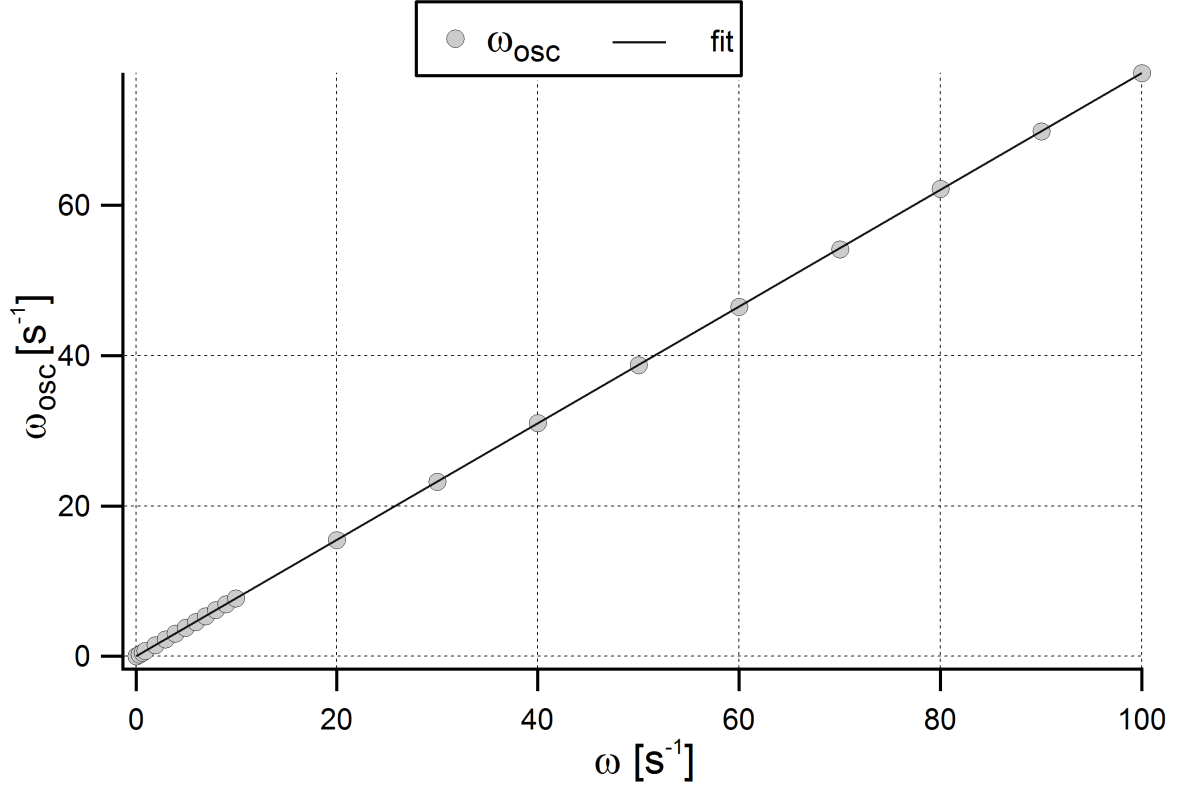


Figure 3.7: Plot of ω_{osc} vs ω (circles) and fit with a line.

Then we fit the data with a line and obtained the following relation:

$$\omega_{osc} = 0.7758 \omega + 0.0011 \text{ s}^{-1}. \quad (3.4)$$

The resulted correlation was 0.999998, therefore the behavior of the oscillation frequency of the system is well reproduced by relation (3.4). This behavior could be predicted by observing that the “force” - in analogy to the dynamics equation, see equation (1.11) - on the order parameter is proportional to ω . It follows that $T \propto 1/\omega$ and therefore $\omega_{osc} \propto \omega$.

3.1.2 Technical details

To obtain the data in Section 3.1.1 we use a “0D Model”, with a “Global ODEs and DAEs” physics. The input function is:

$$f(u, u_t, u_{tt}) = u_{tt} + (\textit{alpha} * \textit{omega}0) * u_t + ((\textit{omega}0)^2) * (A * u + B * (u^3)).$$

In COMSOL Multiphysics we used the variable *omega0* standing for ω of this work and *alpha* standing for α of this work.

The parameters and the initial values used are indicated for each graph.

We use a “Time Dependent Study”, with “Generalized alpha” time stepping method. The steps taken by solver are manual, with time step varying from 1 to 10^{-4} , depending on the frequency we are solving for.

3.2 Time-independent equilibrium order parameter with damping

3.2.1 Results

In the current section we would like to see how the order parameter behaves if the damping coefficient is not negligible. Therefore fix the parameters:

- $A \equiv -1$ (dimensionless), in order to obtain a non-zero order parameter;
- $B \equiv 1$ (dimensionless).

So from equation (1.10) the equilibrium value is:

$$\eta_{eq} = \sqrt{-\frac{A}{B}} = 1.$$

Then in this section we keep fixed the parameter $\omega = 10 \text{ s}^{-1}$ and we analyze the behavior of the order parameter when α changes.

- If we choose $\omega = 10 \text{ s}^{-1}$, $\alpha = 0.05$ as parameters and $\eta|_{t=0} = 1.1$, $\frac{d\eta}{dt}|_{t=0} = 0 \text{ s}^{-1}$ as initial values, we have the following solution:

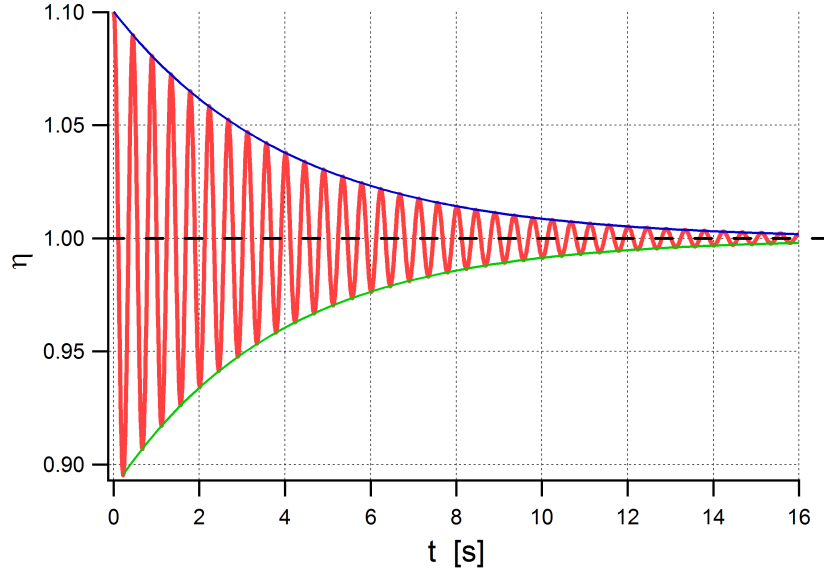


Figure 3.8: Red line: Solution for GL equation in the case of homogeneous in space η , with $\omega = 10 \text{ s}^{-1}$, $\alpha = 0.05$ as parameters and $\eta|_{t=0} = 1.1$, $\frac{d\eta}{dt}|_{t=0} = 0 \text{ s}^{-1}$ as initial values. Green line and blue line: envelope of the order parameter motion.

As you can see in the last figure, the order parameter oscillates around the equilibrium and the amplitude decreases with time.

By analogy to the harmonic oscillator we can say that the system is in an “underdamped” regime.

Fitting the maxima points against time graph with a decreasing exponential (blue line in last picture)

$$\eta_0 + (\delta\eta) \exp(-\gamma t),$$

we obtained the following values:

$$\eta_0 = 0.99978,$$

$$\delta\eta = 0.10044,$$

$$\gamma = 0.24236 \text{ s}^{-1}.$$

The value of γ is about $(\alpha\omega)/2$ and the exponential curve acts as an envelope of the order parameter, in complete analogy to equation (4) of the Appendix.

- If we choose $\omega = 10 \text{ s}^{-1}$, $\alpha = 0.2$ as parameters and $\eta|_{t=0} = 1.1$, $\frac{d\eta}{dt}|_{t=0} = 0 \text{ s}^{-1}$ as initial values, we have the following solution:

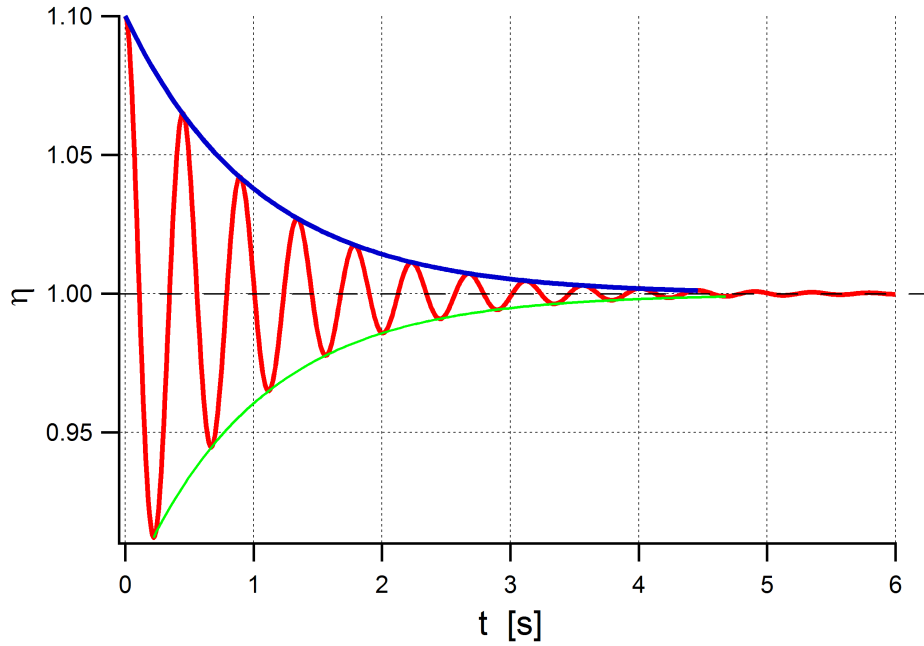


Figure 3.9: Red line: Solution for GL equation in the case of homogeneous in space η , with $\omega = 10 \text{ s}^{-1}$, $\alpha = 0.2$ as parameters and $\eta|_{t=0} = 1.1$, $\frac{d\eta}{dt}|_{t=0} = 0 \text{ s}^{-1}$ as initial values. Green line and blue line: envelope of the motion of the order parameter.

As you can see in the last figure, the order parameter oscillates around the equilibrium value and the amplitude decreases with time.

This case has a damping larger than the previous case, because η reaches the equilibrium value at shorter times, as expected from the choice of a greater α .

By analogy to the harmonic oscillator we can say that the system is in an “underdamped” regime.

Fitting the maxima points of $\eta(t)$ with a decreasing exponential (blue line in last picture)

$$\eta_0 + (\delta\eta) \exp(-\gamma t),$$

we obtained the following values:

$$\eta_0 = 0.99977,$$

$$\delta\eta = 0.10039,$$

$$\gamma = 0.96874 \text{ s}^{-1}.$$

The value of γ is about $(\alpha\omega)/2$ and the exponential curve acts as an envelope of the order parameter, in complete analogy to equation (4) of the Appendix.

The analogy with the damped harmonic oscillator can be justified by the approximations made in last section to obtain equation (3.3).

- Now we choose $\omega = 10 \text{ s}^{-1}$ as parameter, $\eta|_{t=0} = 1.1$, $\frac{d\eta}{dt}|_{t=0} = 0 \text{ s}^{-1}$ as initial values. We let α range from 1.5 to 4 and we obtain the following solutions:

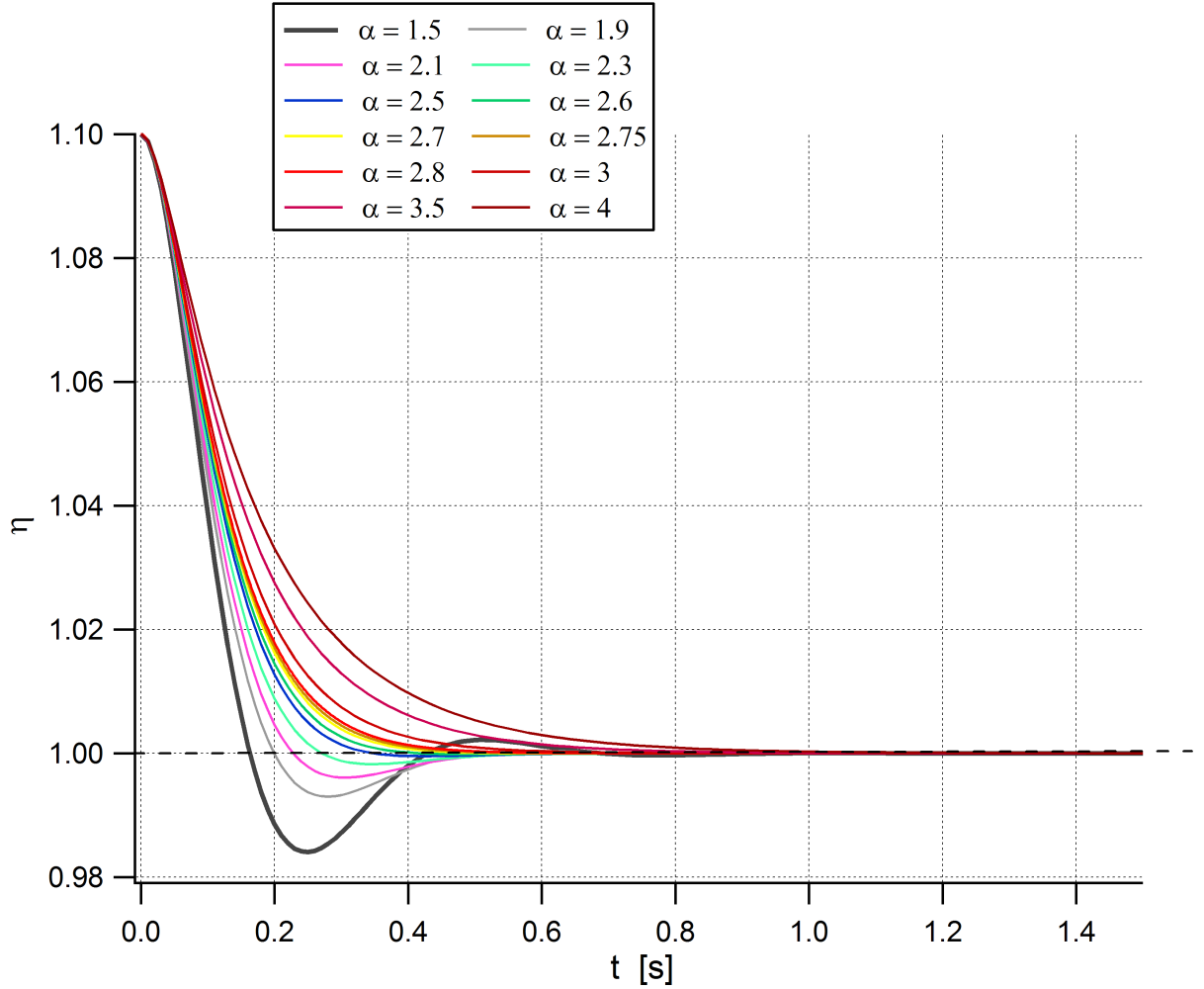


Figure 3.10: Solutions for GL equation in the case of homogeneous in space η , with $\omega = 10 \text{ s}^{-1}$ as parameter and $\eta|_{t=0} = 1.1$, $\frac{d\eta}{dt}|_{t=0} = 0 \text{ s}^{-1}$ as initial values. α ranges from 1.5 to 4.

From last picture we can observe that up to $\alpha = 2.3$ the order parameter falls below the equilibrium value and finally η reaches the equilibrium value. So up to $\alpha = 2.3$ the system is in the “underdamped” regime.

Then we analyze separately the behavior of the solutions for α ranging from 2.5 to 2.8. In particular, expanding the order parameter axis about the

equilibrium value, we obtain the following solutions:

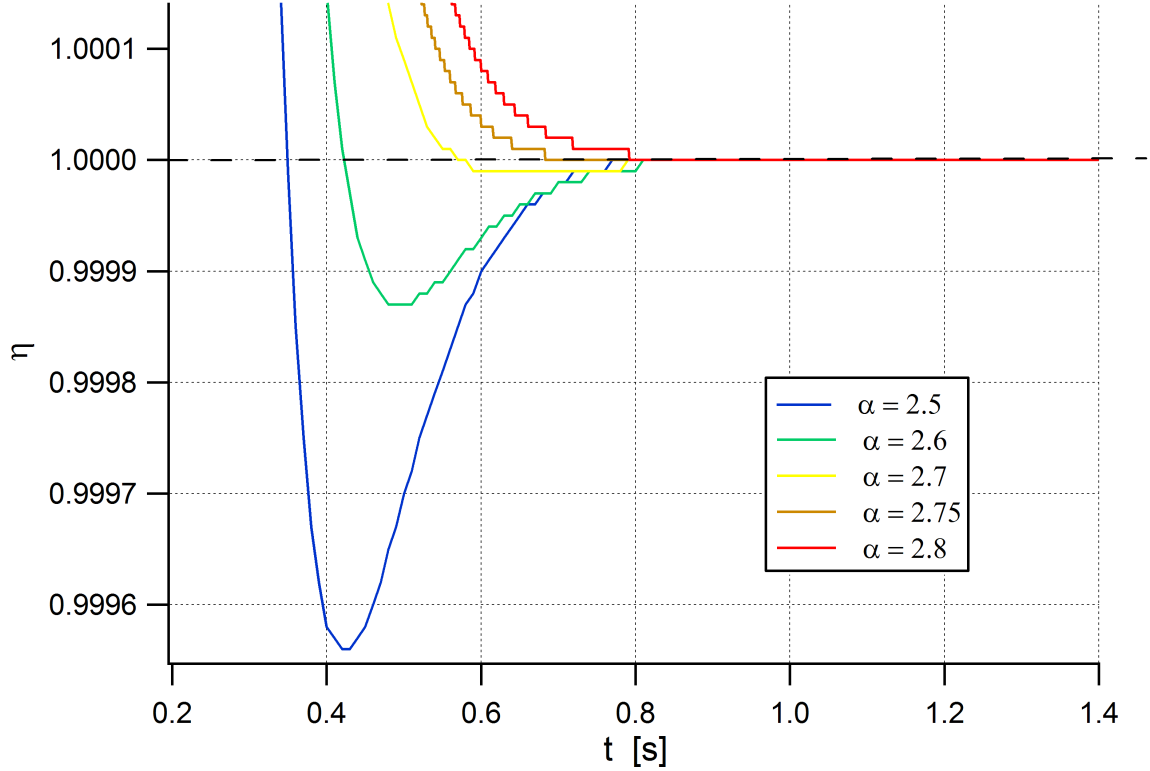


Figure 3.11: Solutions for GL equation in the case of homogeneous in space η , with $\omega = 10 \text{ s}^{-1}$ as parameter and $\eta|_{t=0} = 1.1$, $\frac{d\eta}{dt}|_{t=0} = 0 \text{ s}^{-1}$ as initial values. α ranges from 2.5 to 2.8.

As you can see from the last figure, up to $\alpha = 2.7$ the order parameter falls below the equilibrium value and finally η reaches the equilibrium value. So up to $\alpha = 2.7$ the system is in the “underdamped” regime.

$\alpha = 2.75$ is the first value where the order parameter does not fall below the equilibrium value. So we can argue that at about $\alpha = 2.75$ the system is in *critically damped* regime.

Reminding that choosing $\omega = 10 \text{ s}^{-1}$ the system has an oscillation frequency of $\omega_{osc} = 13.96 \text{ s}^{-1}$, we notice that the case of *critically damped* regime falls when $\alpha\omega$ is about 2 times ω_{osc} , in perfect agreement with the theory of damped harmonic oscillator.

Finally, the cases $\alpha = 3$ and $\alpha = 4$ represent the overdamped harmonic oscillator regime.

3.2.2 Technical details

To obtain the data in Section 3.2.1 we use a “0D Model”, with a “Global ODEs and DAEs” physics. The input function is:

$$f(u, u_t, u_{tt}) = u_{tt} + (\text{alpha} * \text{omega0}) * u_t + ((\text{omega0})^2) * (A * u + B * (u^3)).$$

In COMSOL Multiphysics we used the variable *omega0* standing for ω of this work and *alpha* standing for α of this work.

The parameters and the initial values used are indicated for each graph.

We use a “Time Dependent Study”, with “Generalized alpha” time stepping method. The steps taken by solver are manual, with a time step of 10^{-3} .

3.3 Time-dependent equilibrium order parameter with no damping

3.3.1 Results

In this section we analyze the behavior of the order parameter if the equilibrium value changes with time. Therefore we suppose that for $t < 0$ s the system has the parameters $A = -1$ and $B = 1$, so the order parameter is in equilibrium at the value $\eta = 1$.

Then at time $t = 0$ s a laser pulse hits the system changing the properties. In particular we suppose that the system is brought in another state with another value for the equilibrium parameter, obtained changing the value of A .

Then, for $t > 0$ the system tends to return in the initial state, so the coefficient A can be thought as time dependent.

In this section we choose:

$$A(t) = \begin{cases} -1 & \text{for } t < 0 \text{ s} \\ -1 + de^{-t/\tau} & \text{for } t > 0 \text{ s} \end{cases}$$

with $d < 1$, so the system supports an order parameter; this coefficient is dimensionless.

$$B = 1 \text{ (dimensionless), } \forall t.$$

τ represents the temporal scale for the system to return in the initial state.

We solve GL equation for $t > 0$ s, and the behavior of the order parameter for negative times is represented by choosing $\eta|_{t=0} = 1$, $\frac{d\eta}{dt}|_{t=0} = 0 \text{ s}^{-1}$ as initial values.

We analyze the following cases:

- If we choose $\omega = 0.03 \text{ s}^{-1}$, $\alpha = 0.2$, $d = -0.1$, $\tau = 10^{10} \text{ s}$ as parameters and $\eta|_{t=0} = 1$, $\frac{d\eta}{dt}|_{t=0} = 0 \text{ s}^{-1}$ as initial values, we have the following solution:

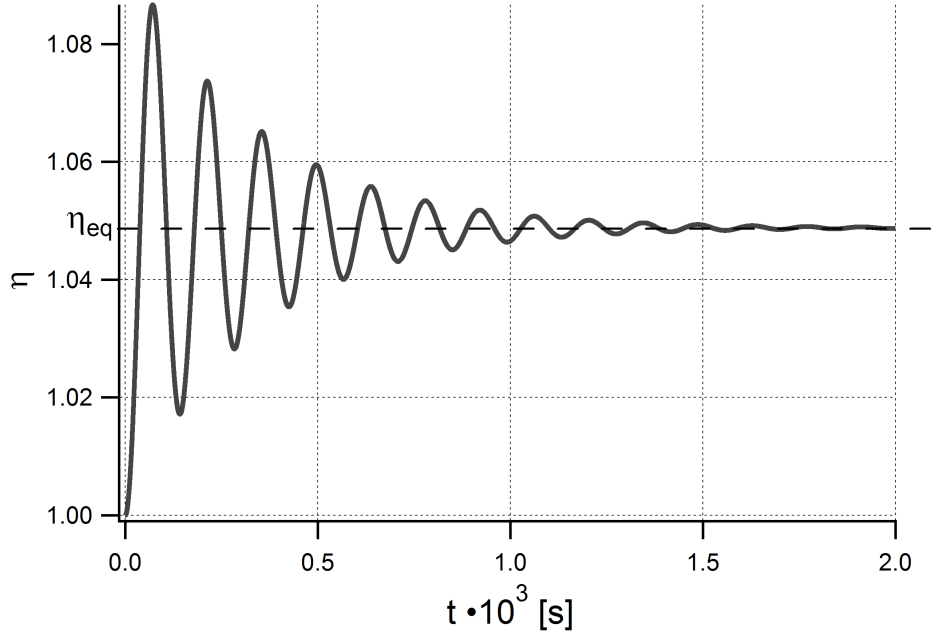


Figure 3.12: Solution for GL equation in the case of homogeneous in space η , with $\omega = 0.03 \text{ s}^{-1}$, $\alpha = 0.2$, $d = -0.1$, $\tau = 10^{10} \text{ s}$ as parameters and $\eta|_{t=0} = 1$, $\frac{d\eta}{dt}|_{t=0} = 0 \text{ s}^{-1}$ as initial values.

Since τ is widely bigger than the solution times, the system returns in the original state for very long times and during the solution times the system does not change state. Therefore this case represents an order parameter starting out of equilibrium and oscillating about:

$$\eta_{eq} = \sqrt{-\frac{A}{B}} = \sqrt{\frac{1.1}{1}} = 1.0488.$$

- If we choose $\omega = 0.03 \text{ s}^{-1}$, $\alpha = 0.2$, $d = 0.1$, $\tau = 1 \text{ s}$ as parameters and $\eta|_{t=0} = 1$, $\frac{d\eta}{dt}|_{t=0} = 0 \text{ s}^{-1}$ as initial values, we have the following solution:

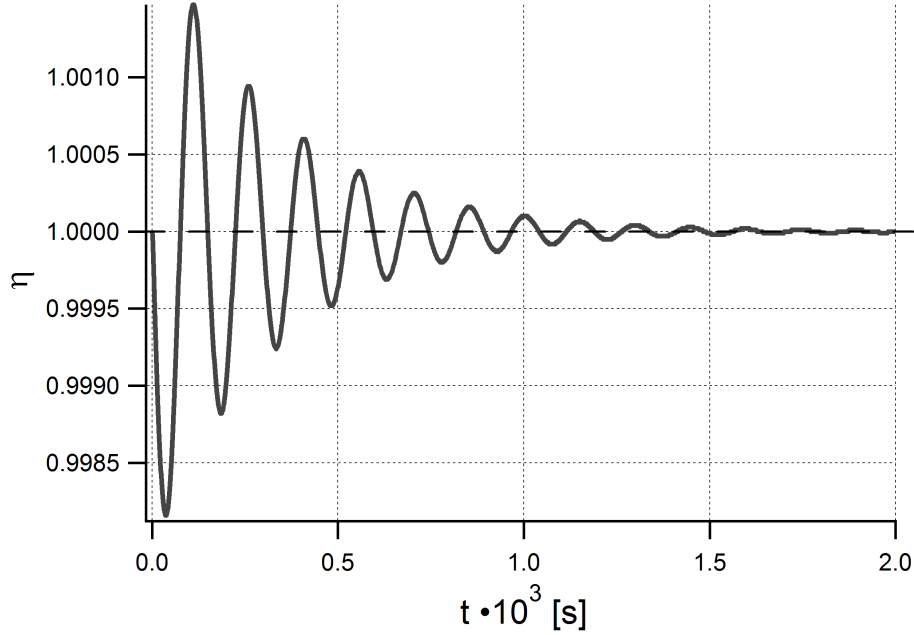


Figure 3.13: Solution for GL equation in the case of homogeneous in space η , with $\omega = 0.03 \text{ s}^{-1}$, $\alpha = 0.2$, $d = 0.1$, $\tau = 1 \text{ s}$ as parameters and $\eta|_{t=0} = 1$, $\frac{d\eta}{dt}|_{t=0} = 0 \text{ s}^{-1}$ as initial values.

At the beginning, η is out of equilibrium, because:

$$\eta_{eq, \text{ beginning}} = \sqrt{-\frac{A}{B}} = \sqrt{\frac{0.9}{1}} = 0.9487.$$

So the order parameter initially moves towards $\eta_{eq, \text{ beginning}}$.

Since τ is widely smaller than the solution times, after few seconds the system returns in the original state, with $\eta_{eq} = 1$. Therefore after some seconds the order parameter moves from $\eta_{eq, \text{ beginning}}$ towards $\eta_{eq} = 1$, like the case of an order parameter out of equilibrium.

- If we choose $\omega = 0.03 \text{ s}^{-1}$, $\alpha = 0.2$, $d = -0.1$, $\tau = 200 \text{ s}$ as parameters and $\eta|_{t=0} = 1$, $\frac{d\eta}{dt}|_{t=0} = 0 \text{ s}^{-1}$ as initial values, we have the following solution:

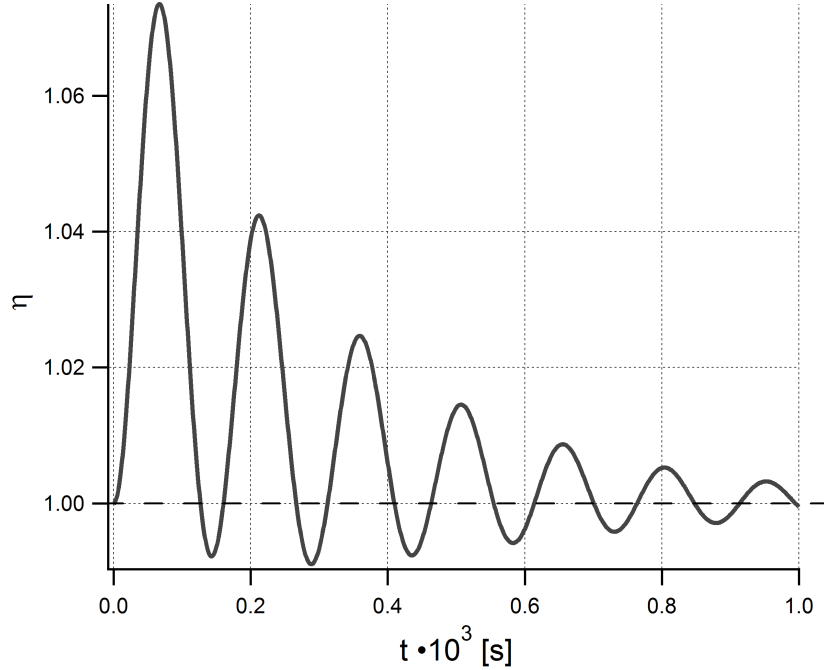


Figure 3.14: Solution for GL equation in the case of homogeneous in space η , with $\omega = 0.03 \text{ s}^{-1}$, $\alpha = 0.2$, $d = -0.1$, $\tau = 200 \text{ s}$ as parameters and $\eta|_{t=0} = 1$, $\frac{d\eta}{dt}|_{t=0} = 0 \text{ s}^{-1}$ as initial values.

At the beginning, η is out of equilibrium, because:

$$\eta_{eq, \text{beginning}} = \sqrt{-\frac{A}{B}} = \sqrt{\frac{1.1}{1}} = 1.0488.$$

So the order parameter initially oscillates about $\eta_{eq, \text{beginning}}$.

Finally, when the time is widely larger than τ the system returns in the original state, with $\eta_{eq} = 1$. Therefore for long times η oscillates about $\eta_{eq} = 1$, like the case of an order parameter out of equilibrium.

This is an intermediate case with respect to the two previous limiting cases.

3.3.2 Technical details

To obtain the data in Section 3.3.1 we use a “0D Model”, with a “Global ODEs and DAEs” physics. The input function is:

$$f(u, u_t, u_{tt}) = u_{tt} + (\text{alpha} * \text{omega0}) * u_t + ((\text{omega0})^2) * (A * u + B * (u^3)),$$

with:

$$A = A0 * (1 - d * \exp(-t/\text{tau})).$$

$A0 = -1$ fixed.

In COMSOL Multiphysics we used the variable omega0 standing for ω of this work, alpha standing for α of this work and tau standing for τ of this work.

The parameters and the initial values used are indicated for each graph.

We use a “Time Dependent Study”, with “Generalized alpha” time stepping method. The steps taken by solver are manual, with a time step of 10^{-3} for the case with $\tau = 10^{10}$ s, of 1 for the case with $\tau = 1$ s and of 0.1 for the case with $\tau = 200$ s.

References

1. Massimo Capone, Michele Fabrizio, Daniele Fausti, Claudio Giannetti, Fulvio Parmigiani, *Ultrafast optical spectroscopy of strongly-correlated materials and high-temperature superconductors: a non-equilibrium approach*, Advances in Physics Vol. 00, No. 00, June 2008, 1-36.

Chapter 4

Reflectivity for a system in overdamped regime

In this chapter we simulate a cylindrical system, brought out of equilibrium by a laser pulse, and we discuss the dynamics of the order parameter. We suppose that the energy received from the laser pulse is diffused in the system and then given to the thermal bath surrounding the cylinder. Therefore we have to deal with an overdamped regime, in which the propagation of the order parameter is incoherent.

Finally we use simulations data to reproduce reflectivity behavior of a superconductor sample.

In this chapter we try to solve numerically GL equation for real order parameter:

$$\frac{1}{\omega^2} \frac{\partial^2 \eta}{\partial t^2} + \left(\frac{\alpha}{\omega} \right) \frac{\partial \eta}{\partial t} + A(P, T)\eta + B(P)\eta^3 - \lambda \nabla^2 \eta = 0$$

using “COMSOL Multiphysics” software, in the case of an overdamped system. Therefore we choose the following parameters:

- $\omega = 10 \text{ s}^{-1}$;
- $\alpha = 10^3$ (dimensionless), so the term of the second derivate with respect to time becomes negligible with respect to the term of the first derivate. This condition makes the overdamped regime;
- $\lambda = 0.1 \text{ m}^2$;
- $A = -1$ (dimensionless), so the system supports an order parameter;
- $B = 1$ (dimensionless).

The analyzed system is a cylinder with a radius of 2 m and a thickness $d = 0.3$ m.

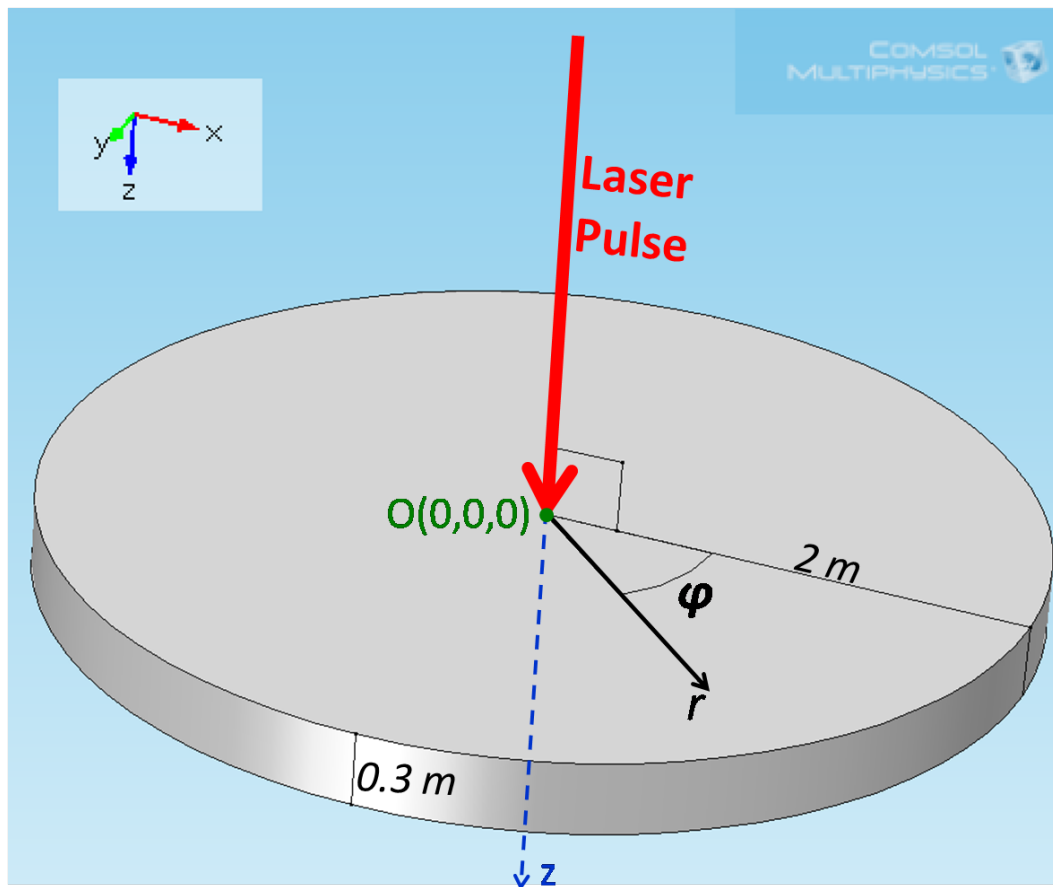


Figure 4.1: The analyzed system.

The origin of the coordinates is chosen as the center of one base, with reference to the last figure. For the shape of the analyzed sample, it is useful to use a system of cylindrical coordinates (r, φ, z) , as indicated in last picture.

To solve GL equation, we apply “zero flux” (i.e. $\nabla\eta = 0$) boundary condition on all the external surface. This boundary condition implies that the order parameter is constant at the external surface and that there is no current of order parameter through the external surface.

Actually this boundary condition is not true in experiments, because outside of the system there is vacuum and so the order parameter should diminish and go to 0 near the boundaries.

However we choose zero flux boundary condition because it is very easy to implement and to obtain a solution; furthermore it is a good approximation to reality for the initial times, when the perturbation of order parameter has not reached the boundaries yet.

With this condition the order parameter at equilibrium is $\eta_{eq} \equiv 1$ over all the system.

For negative times $t < 0$ s we suppose that a laser pulse hits the base with coordinate $z = 0$ m and excites the system, as depicted in figure 4.1. Then at time $t = 0$ s the laser pulse is turned off, so that the initial values for the order parameter are:

$$\eta|_{t=0} = 1 - I \exp\left(-\frac{z}{l_{pen}}\right) \exp\left(-\frac{r^2}{l_{width}^2}\right); \quad (4.1)$$

$$\left.\frac{d\eta}{dt}\right|_{t=0} = 0 \text{ s}^{-1}. \quad (4.2)$$

Initial value (4.1) tells us that for negative times ($t < 0$ s) a laser pulse adds a perturbation to the equilibrium order parameter ($\eta_{eq} \equiv 1$).

The laser pulse hits the system on the base with coordinate $z = 0$ m and the perturbation decreases exponentially as we go inside the sample. l_{pen} represents the spatial scale over which the order parameter returns to the equilibrium value. The perturbation has a rotational symmetry, so we can use a 2D-axisymmetric geometry and study the behavior of the order parameter on a half-plane (r, z) with φ fixed. Thanks to this symmetry, it does not matter the choice of the particular value of φ .

The perturbation has and a gaussian shape, with the z axis as center and l_{width} as width.

In this chapter we analyze the behavior of the system for different values of l_{pen} and of the parameter I (representing the intensity of the laser pulse), while we will hold fixed the parameter $l_{width} = 0.5$ m.

Initial value (4.2) means that the laser pulse brings the system in another equilibrium state. So the system does not move until the laser is turned off (at $t = 0$ s) and at $t = 0$ s the order parameter as a negligible “velocity” (in analogy to the dynamics equation).

For $t > 0$ s the system moves towards the equilibrium state with $\eta = \eta_{eq} \equiv 1$.

When the order parameter in a certain point of the system changes, the reflectivity (R) in that point changes.

In particular, introducing $\delta\eta = \eta - \eta_{eq}$ (as explained in section 1.4), we can assume that the following relation holds:

$$R = \gamma |\delta\eta|, \quad (4.3)$$

where γ is a constant.

This relation allows us to predict the reflectivity of the system behavior when we know $\delta\eta$.

After analyzing the behavior of the order parameter in some interesting case, in this chapter we compare experimental reflectivities with data from the solution of GL equation, obtained with COMSOL Multiphysics.

4.1 Results

4.1.1 Homogeneous excitation

This case is when l_{pen} is larger than the thickness of the system in the z direction; therefore $\delta\eta$ is almost equal in z direction at the initial times.

In particular we solved GL equation for the case $l_{pen} = 100$ m (we remind that the thickness of the system in z direction is $d = 0.3$ m).

Letting I assume several values, we analyze a few cases. For each value of the parameter I we make a simulation.

Choosing $I = 0$ (i.e. no laser applied for $t < 0$ s), we verify that the system stays forever in the equilibrium value $\eta_{eq} \equiv 1$:

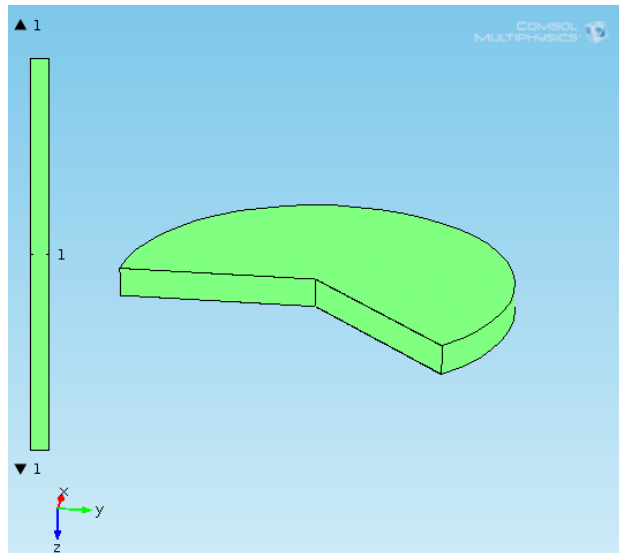


Figure 4.2: The solution for $l_{pen} = 100$ m and $I = 0$, for all times. The color scale represents the value of η .

Since $I = 0$, we can notice that this result does not depend on the particular choice of l_{pen} .

Choosing $I = 0.8$ the order parameter changes so:

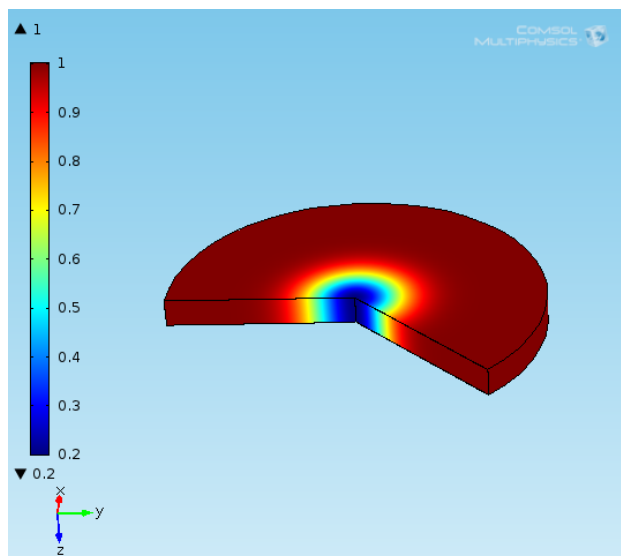


Figure 4.3: The solution for $l_{pen} = 100$ m and $I = 0.8$, for $t = 0$ s. The color scale represents the value of η .

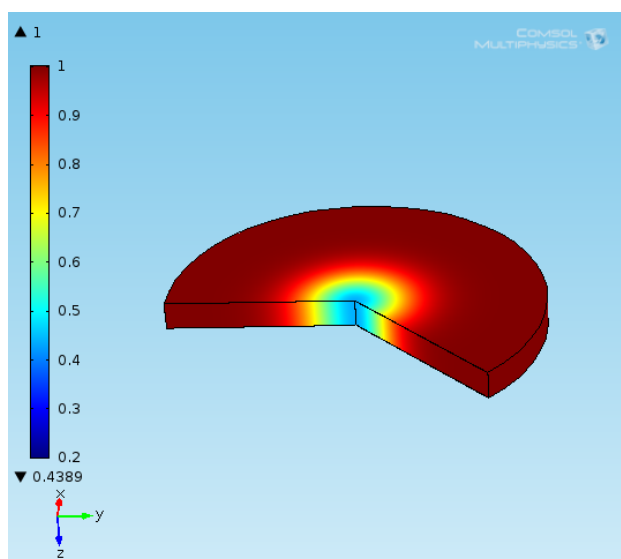


Figure 4.4: The solution for $l_{pen} = 100$ m and $I = 0.8$, for $t = 30$ s. The color scale represents the value of η .

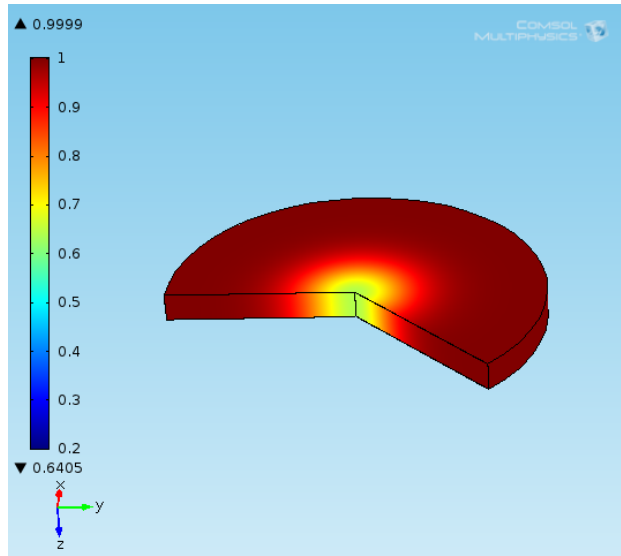


Figure 4.5: The solution for $l_{pen} = 100$ m and $I = 0.8$, for $t = 60$ s. The color scale represents the value of η .

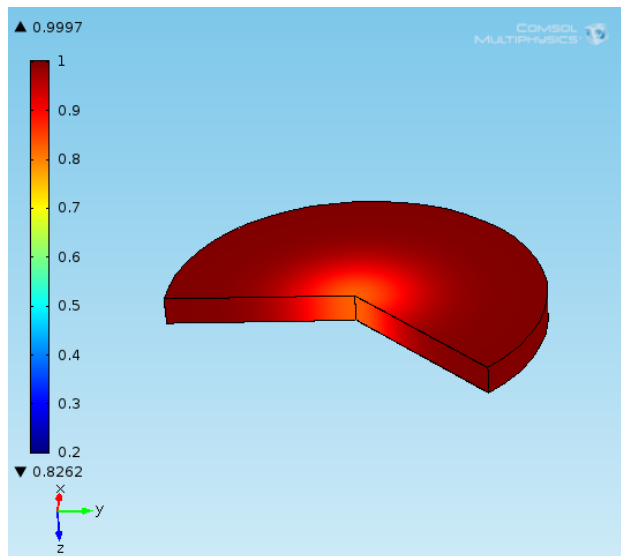


Figure 4.6: The solution for $l_{pen} = 100$ m and $I = 0.8$, for $t = 100$ s. The color scale represents the value of η .

As you can see from figures 4.3 - 4.6, as time passes the order parameter tends to return the equilibrium value ($\eta_{eq} \equiv 1$), without making oscillation about η_{eq} .

This behavior is typical of the overdamped regime.

We can also note that the order parameter is actually constant in z direction. In this particular case the equation reduces to a diffusion equation.

When the intensity of laser pulse increases and is greater than 1, the initial value described by (4.1) is no more correct because this would imply a negative order parameter in a certain domain at $t = 0$ s. For a fixed φ , in the half-plane (r, z) the order parameter would be positive in Ω_1 domain and negative in Ω_2 domain, with reference to figure 4.7.

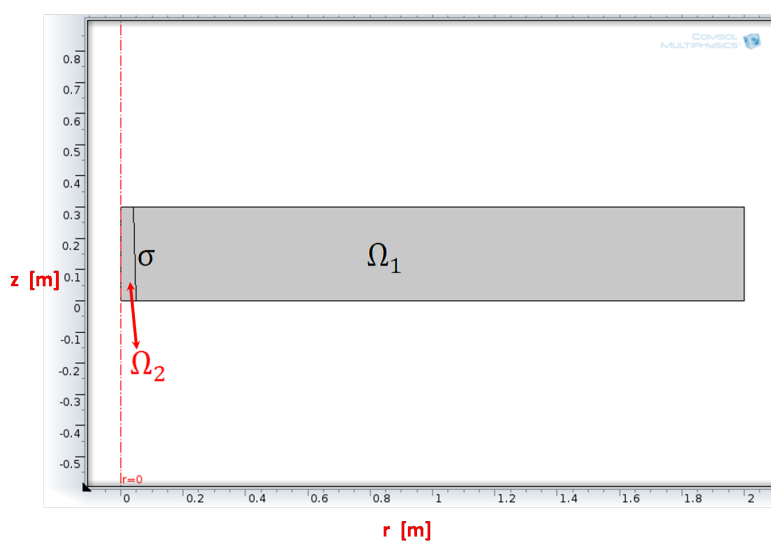


Figure 4.7: The half-plane (r, z) , for a fixed φ .

σ would be the line where the order parameter is 0. So from condition (4.1):

$$I \exp\left(-\frac{z}{l_{pen}}\right) \exp\left(-\frac{r^2}{l_{width}^2}\right) = 1.$$

Taking the logarithm we have:

$$\frac{z}{l_{pen}} + \frac{r^2}{l_{width}^2} = \ln I,$$

and this can be written as:

$$z = -\left(\frac{l_{pen}}{l_{width}^2}\right) r^2 + (\ln I) l_{pen}. \quad (4.4)$$

So we proved that σ is defined by (4.4), which is the equation of a parabola.

Therefore we split the half-plane (r, z) in 2 domains, defined in figure 4.7 and by relation (4.4), and we apply the following initial values condition:

$$\eta|_{t=0} = \begin{cases} 1 - I \exp\left(-\frac{z}{l_{pen}}\right) \exp\left(-\frac{r^2}{l_{width}^2}\right) & \text{for } (r, z) \text{ in } \Omega_1 \\ 0 & \text{for } (r, z) \text{ in } \Omega_2 \end{cases} \quad (4.5)$$

$$\left. \frac{d\eta}{dt} \right|_{t=0} = 0 \quad \text{s}^{-1} \quad \text{everywhere.} \quad (4.6)$$

With this condition we analyze a few cases with a high intensity laser.

Now we would like to evaluate the reflectivity of the system in the region where the laser effects are high. To obtain this, we make an average of the order parameter along a line, defined by the coordinate $r = 0$ m (where there is the center of the gaussian pulse). The line starts at $z = 0$ m and is not longer than l_{pen} (in this region the laser effects are high).

In the particular case of the current section, where the height of the cylinder d is much shorter than l_{pen} , z coordinate of the average line ranges from the beginning to the end of the cylinder.

Finally, to obtain $|\langle \delta\eta \rangle|$ (the average of $\delta\eta$ with positive sign), we subtract $\eta_{eq} \equiv 1$ to the average order parameter and take the positive sign.

$|\langle \delta\eta \rangle|$ is a function of the laser intensity I and of the time.

From the definitions above, we are able to evaluate the expression of $|\langle \delta\eta \rangle|$ at $t = 0$ s analytically.

As stated before, we make the average on a line ranging from $z = 0$ m to $z = w$ (we use w to cover all the possible cases: w can be either the end of the cylinder d or l_{pen}). Using relations (4.1), (4.4) and (4.5) we have 3 different cases:

- $I \leq 1$. In this case relation (4.1) holds over all the average line:

$$\begin{aligned} |\langle \delta\eta(t = 0 \text{ s}) \rangle| &= |\langle \eta(t = 0 \text{ s}) - \eta_{eq} \rangle| = \\ &= \left| \frac{1}{w} \int_0^w [\eta(t = 0 \text{ s}, r = 0 \text{ m}, z) - \eta_{eq}] dz \right| = \end{aligned}$$

$$= \left| \frac{I}{w} \int_0^w \exp\left(-\frac{z}{l_{pen}}\right) dz \right| = \frac{l_{pen}}{w} \left[1 - \exp\left(-\frac{w}{l_{pen}}\right) \right] I. \quad (4.7)$$

- $1 < I \leq \exp(w/l_{pen})$. In this case the average line lies in 2 domains (the average line lies completely in Ω_1 domain at the limit value $I = \exp(w/l_{pen})$), so we have to make the average using relation (4.5):

$$\begin{aligned} |\langle \delta\eta(t=0 \text{ s}) \rangle| &= |\langle \eta(t=0 \text{ s}) - \eta_{eq} \rangle| = \\ &= \left| \frac{1}{w} \int_0^w [\eta(t=0 \text{ s}, r=0 \text{ m}, z) - \eta_{eq}] dz \right| = \\ &= \left| -\frac{1}{w} \int_0^{(\ln I)l_{pen}} dz - \frac{I}{w} \int_{(\ln I)l_{pen}}^w \exp\left(-\frac{z}{l_{pen}}\right) dz \right| = \\ &= \left| -\frac{(\ln I)l_{pen}}{w} + \frac{l_{pen}I}{w} \left\{ \exp\left(-\frac{w}{l_{pen}}\right) - \exp\left[-\frac{(\ln I)l_{pen}}{l_{pen}}\right] \right\} \right| = \\ &= \frac{l_{pen}}{w} \left| 1 + (\ln I) - I \exp\left(-\frac{w}{l_{pen}}\right) \right| = \\ &= \frac{l_{pen}}{w} \left[1 + (\ln I) - I \exp\left(-\frac{w}{l_{pen}}\right) \right]. \quad (4.8) \end{aligned}$$

The last equality follows from the fact that in this range of intensity, $I \exp(-w/l_{pen})$ ranges from 0 to 1 and so

$$1 + (\ln I) - I \exp(-w/l_{pen})$$

is always positive.

In the case of $I \rightarrow 1$ expression (4.8) reduces to expression (4.7). Therefore the general expression of $|\langle \delta\eta \rangle|$ is continuous at $I = 1$.

Evidently expression (4.8) increases, reaching the limiting value of 1 if $I \rightarrow \exp(w/l_{pen})$.

- $I > \exp(w/l_{pen})$. In this case the average line lies completely in Ω_1 domain. Therefore:

$$\begin{aligned} |\langle \delta\eta(t=0 \text{ s}) \rangle| &= |\langle \eta(t=0 \text{ s}) - \eta_{eq} \rangle| = \\ &= \left| \frac{1}{w} \int_0^w [\eta(t=0 \text{ s}, r=0 \text{ m}, z) - \eta_{eq}] dz \right| = \left| -\frac{1}{w} \int_0^w dz \right| = 1. \quad (4.9) \end{aligned}$$

This case is reached when the laser is so intense that the order parameter has been brought to 0 over all the average line (saturation).

Increasing the laser intensity, $\delta\eta$ does not change further over the average line.

Evidently the general expression of $|\langle \delta\eta \rangle|$ is continuous at

$$I = \exp(w/l_{pen}).$$

Consequently we have just obtained a continuous expression for $|\langle \delta\eta \rangle|$ at $t = 0$ s:

$$|\langle \delta\eta(t = 0 \text{ s}) \rangle| = \begin{cases} \frac{l_{pen}}{w} \left[1 - \exp\left(-\frac{w}{l_{pen}}\right) \right] I & (4.7) \text{ for } I \leq 1 \\ \frac{l_{pen}}{w} \left| 1 + (\ln I) - I \exp\left(-\frac{w}{l_{pen}}\right) \right| & (4.8) \text{ for } 1 < I \leq \exp\left(\frac{w}{l_{pen}}\right) \\ 1 & (4.9) \text{ for } I > \exp\left(\frac{w}{l_{pen}}\right). \end{cases}$$

As you can see, for $t = 0$ s and $w = l_{pen}$ (laser penetration lower than the cylinder thickness), $|\langle \delta\eta \rangle|$ does not depend on the particular choice of l_{pen} .

Furthermore it is worth to notice that the general expression of $|\langle \delta\eta \rangle|$ is always continuous for every laser intensity.

Now we make a few simulations changing the value of I and for each value of I we evaluate the line average. Here we report the results obtained:

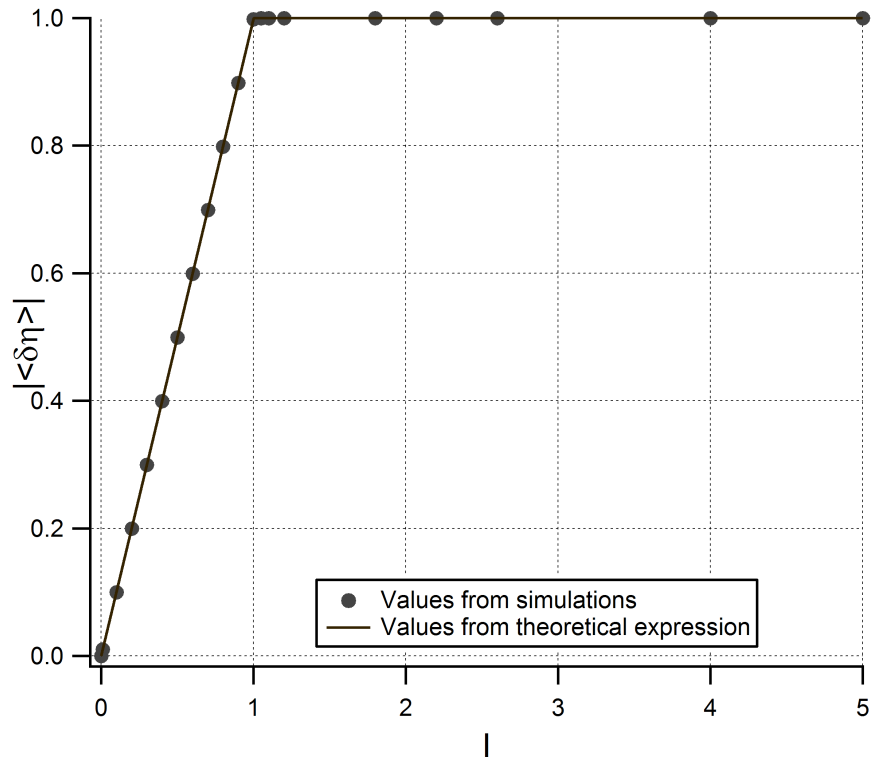


Figure 4.8: Plot of $|\langle \delta\eta \rangle|$ as a function of the laser intensity I , for the initial time $t = 0$ s and $l_{pen} = 100$ m. Here we report the values obtained from the simulations (markers) and the values obtained with the theoretical expression (continuous line).

As you can see from figure 4.8, the values from simulations follow very well the theoretical equation, calculated for $w = d = 0.3$ m (the width of the cylinder). When the intensity grows from 0 to 1, $|\langle \delta\eta \rangle|$ increases proportionally, as predicted by equation (4.7). The theoretical coefficient of proportionality is 0.998501.

As time passes, the order parameter tends to return to the equilibrium value. So the values of $|\langle \delta\eta \rangle|$ diminish with time. The more is the intensity used, the more the system is perturbed and the more time is necessary to return to the equilibrium value (see figure 4.9).

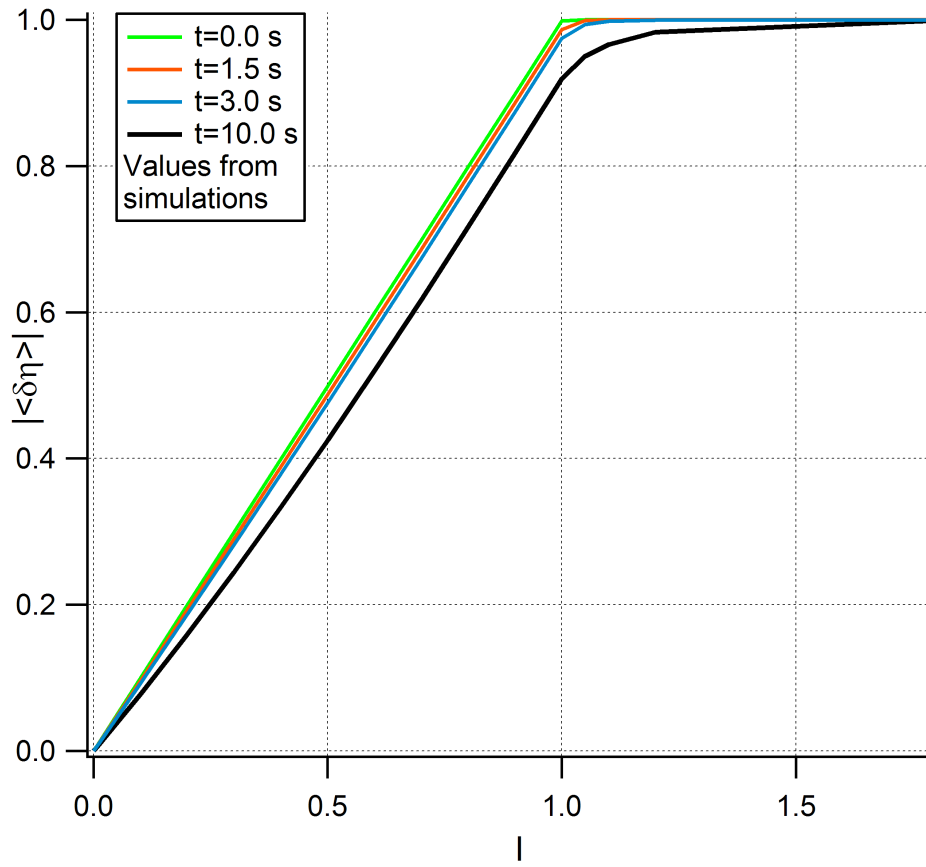


Figure 4.9: Plot of $|\langle \delta\eta \rangle|$ as a function of the laser intensity I , for different times and $l_{pen} = 100$ m. These results are obtained from simulations.

4.1.2 Quasi-homogeneous excitation

In this case l_{pen} is slightly bigger than the thickness of the system in the z direction (d); so $\delta\eta$ is not equal in z direction at the initial times, but $\delta\eta$ varies slightly in z direction.

In particular we solved GL equation for the case $l_{pen} = 1$ m (we remind that the largeness of the system in z direction used is 0.3 m).

Letting I assume several values, we analyze a few cases, using the same criterion expressed in Section 4.1.1.

Choosing $I = 1.15$ the order parameter moves so:

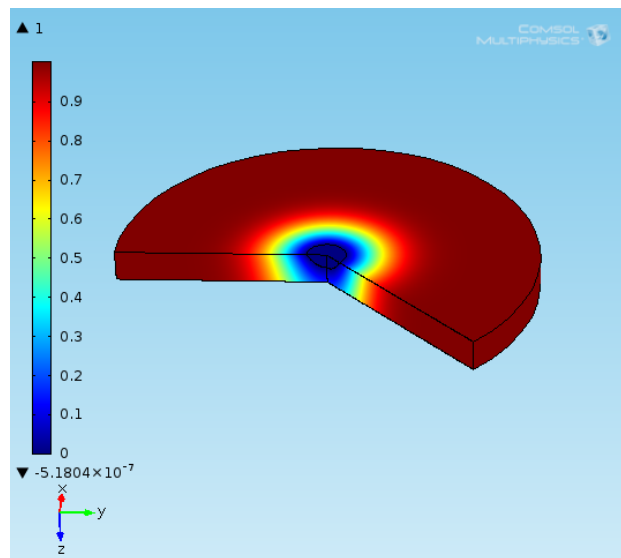


Figure 4.10: The solution for $l_{pen} = 1$ m and $I = 1.15$, for $t = 0$ s. The color scale represents the value of η .

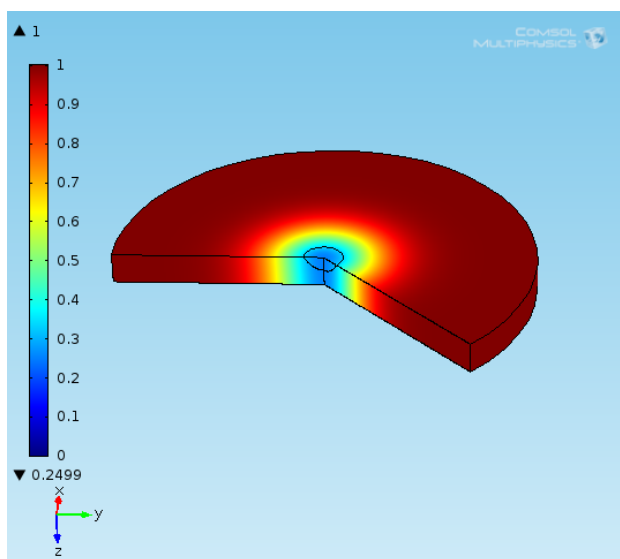


Figure 4.11: The solution for $l_{pen} = 1$ m and $I = 1.15$, for $t = 30$ s. The color scale represents the value of η .

As you can see from figures 4.10 - 4.11, as time passes the order parameter tends to return to the equilibrium value ($\eta_{eq} \equiv 1$), without making oscillation about η_{eq} . This behavior is typical of the overdamped regime.

We can also note that the order parameter does not have significative variations in z direction.

As anticipated in Section 4.1.1, we would like to evaluate the reflectivity of the system in the region where the laser effects are high. To obtain this, we make an average of the order parameter along a line, starting at $(r = 0$ m, $z = 0$ m) and finishing at $(r = 0$ m, $z = w$).

In the particular case of the current section, where the thickness d of the cylinder is shorter than l_{pen} , we choose $w = d$.

As for $|\langle \delta\eta \rangle|$, all the considerations expressed in Section 4.1.1 holds.

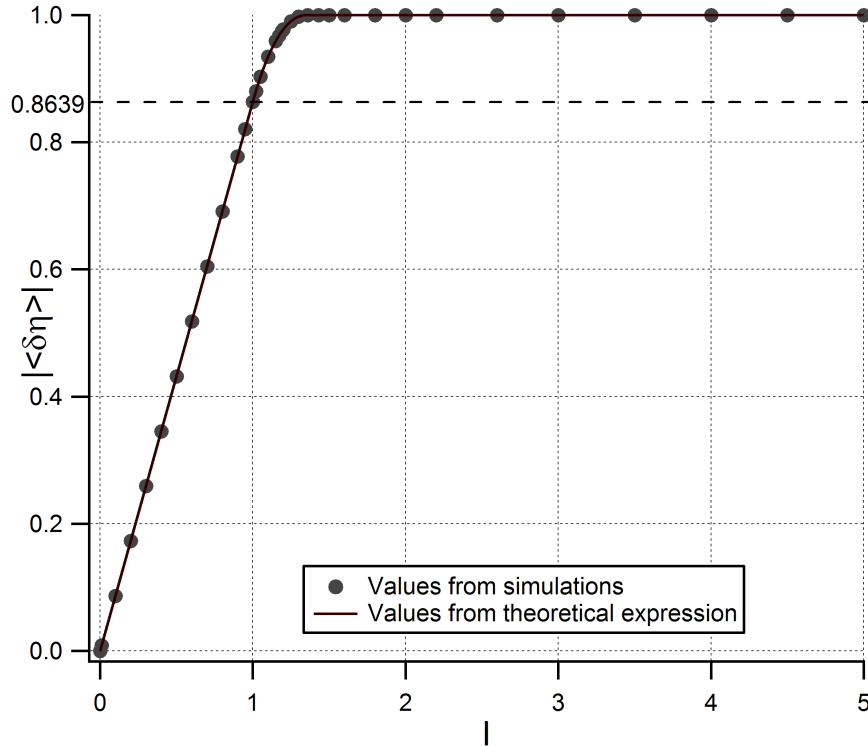


Figure 4.12: Plot of $|\langle \delta\eta \rangle|$ as a function of the laser intensity I , for the initial time $t = 0$ s and $l_{pen} = 1$ m. Here we report the values obtained from the simulations (markers) and the values obtained with the theoretical expression (continuous line).

As you can see from figure 4.12, the values from simulations follow very well the theoretical equation, calculated for $w = d = 0.3$ m (the width of the cylinder). When the intensity grows from 0 to 1, $|\langle \delta\eta \rangle|$ increases proportionally, as predicted by equation (4.7). The theoretical coefficient of proportionality is 0.863939.

As time passes, the order parameter tends to return to the equilibrium value. So the values of $|\langle \delta\eta \rangle|$ diminish with time. The more is the intensity used, the more the system is perturbed and the more time is necessary to return to the equilibrium value (see figure 4.13).

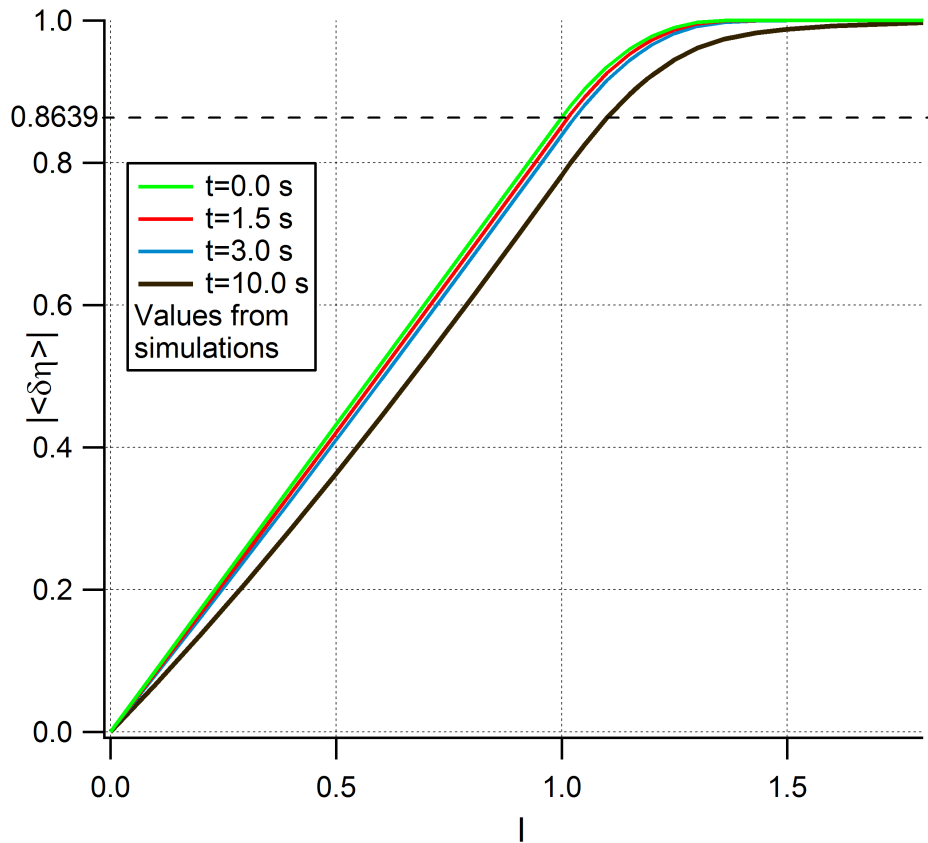


Figure 4.13: Plot of $|\langle \delta\eta \rangle|$ as a function of the laser intensity I , for different times and $l_{pen} = 1$ m. These results are obtained from simulations.

4.1.3 Strongly inhomogeneous excitation

In this case l_{pen} is shorter than the thickness of the system in the z direction (d); so $\delta\eta$ varies a lot in z direction, reaching the value of 0 near one end of the cylinder. Therefore this case is representative of the bulk system, in which the laser does not penetrate in the system.

In particular we solved GL equation for the case $l_{pen} = 0.1$ m (we remind that the largeness of the system in z direction used is $d = 0.3$ m).

Letting I assume several values, we analyze a few cases, using the same criterion expressed in Section 4.1.1.

Choosing $I = 1.5$ the order parameter moves so:

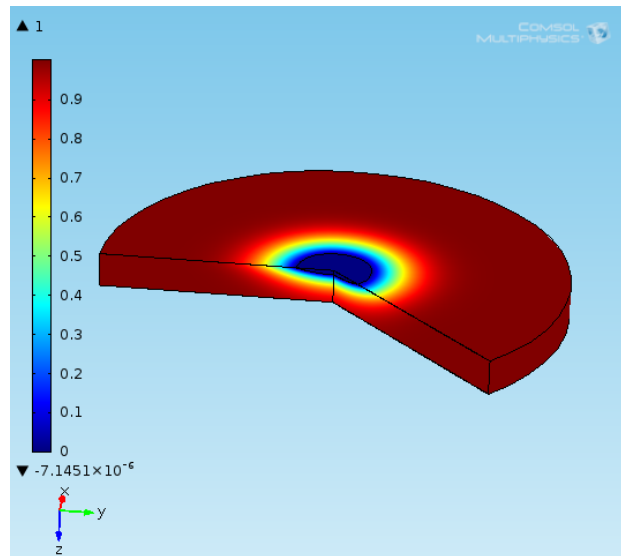


Figure 4.14: The solution for $l_{pen} = 0.1$ m and $I = 1.5$, for $t = 0$ s. The color scale represents the value of η .

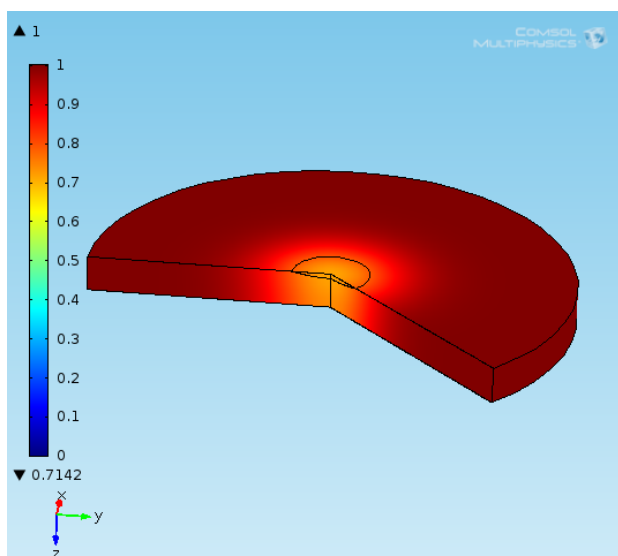


Figure 4.15: The solution for $l_{pen} = 0.1$ m and $I = 1.5$, for $t = 30$ s. The color scale represents the value of η .

As you can see from figures 4.14 - 4.15, as time passes the order parameter tends to return the equilibrium value ($\eta_{eq} \equiv 1$), without making oscillation about η_{eq} . This behavior is typical of the overdamped regime.

We can also note that the order parameter has a big variation in z direction, up to a factor 10. The laser perturbation on a surface weakly influences the system at a depth larger than l_{pen} .

As anticipated in Section 4.1.1, we would like to evaluate the reflectivity of the system in the region where the laser effects are high. To obtain this, we make an average of the order parameter along a line, starting at ($r = 0$ m, $z = 0$ m) and finishing at ($r = 0$ m, $z = w$).

In the particular case of the current section, where the thickness d of the cylinder is longer than l_{pen} , we choose $w = l_{pen}$.

As for $|\langle \delta\eta \rangle|$, all the considerations expressed in Section 4.1.1 holds.

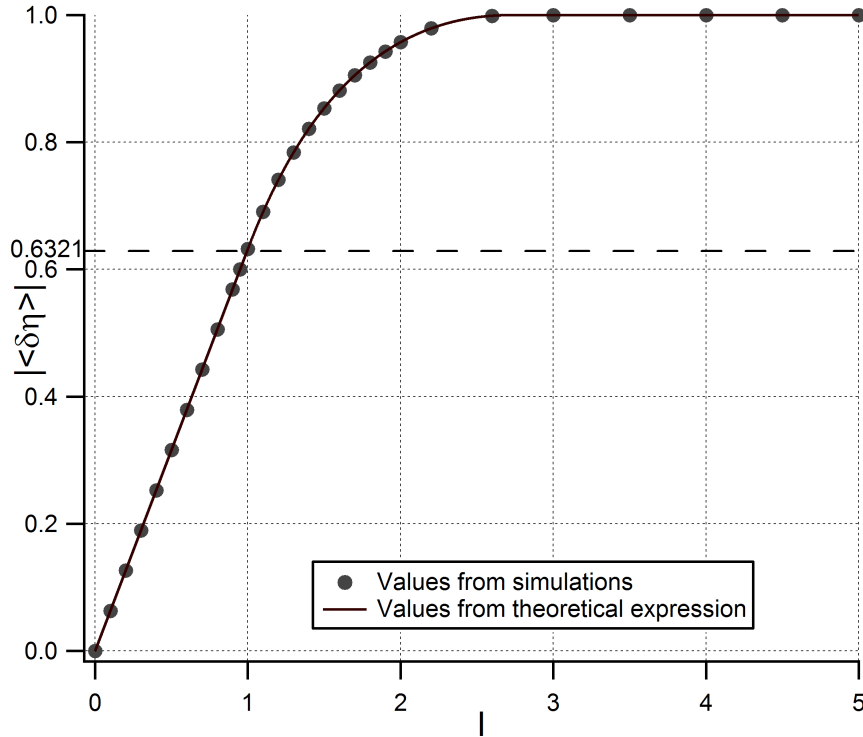


Figure 4.16: Plot of $|\langle \delta\eta \rangle|$ as a function of the laser intensity I , for the initial time $t = 0$ s and $l_{pen} = 0.1$ m. Here we report the values obtained from the simulations (markers) and the values obtained with the theoretical expression (continuous line).

As you can see from figure 4.16, the values from simulations follow very well the theoretical equation, calculated for $w = l_{pen} = 0.1$ m.

When the intensity grows from 0 to 1, $|\langle \delta\eta \rangle|$ increases proportionally, as predicted by equation (4.7). The theoretical coefficient of proportionality is 0.632121.

As time passes, the order parameter tends to return to the equilibrium value. So the values of $|\langle \delta\eta \rangle|$ diminish with time. The more is the intensity used, the more the system is perturbed and the more time is necessary to return to the equilibrium value (see figure 4.17).

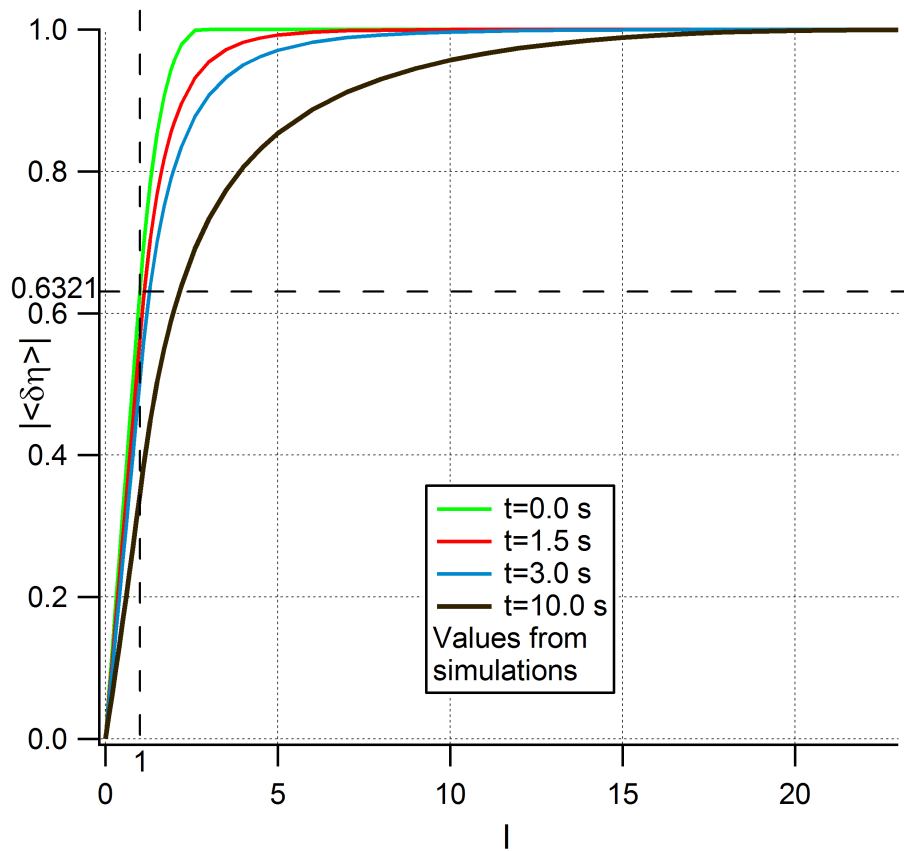


Figure 4.17: Plot of $|\langle \delta\eta \rangle|$ as a function of the laser intensity I , for different times and $l_{pen} = 0.1$ m. These results are obtained from simulations.

4.1.4 Bulk system

In this case l_{pen} is much shorter than the thickness of the system in the z direction (d); so at the initial time $\delta\eta$ varies a lot in z direction, reaching a value close to 0 inside the cylinder. Therefore in this case we have the bulk system.

In particular we solved GL equation for the case $l_{pen} = 0.03$ m (we remind that the thickness of the system in z direction used is $d = 0.3$ m).

Letting I assume several values, we analyze a few cases, using the same criterion expressed in Section 4.1.1.

Choosing $I = 2.6$ the order parameter moves so:

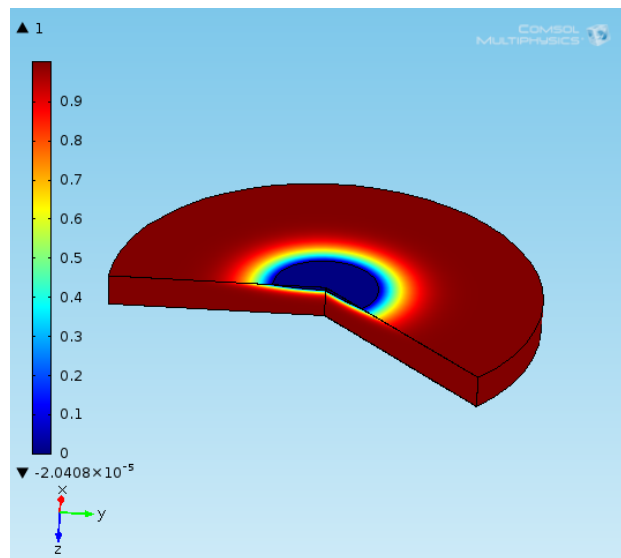


Figure 4.18: The solution for $l_{pen} = 0.03$ m and $I = 2.6$, for $t = 0$ s. The color scale represents the value of η .

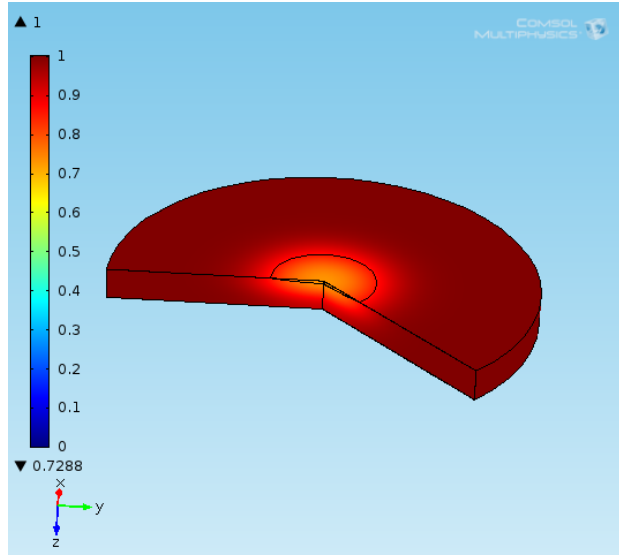


Figure 4.19: The solution for $l_{pen} = 0.03$ m and $I = 2.6$, for $t = 10$ s. The color scale represents the value of η .

As you can see from figures 4.18 - 4.19, as time passes the order parameter tends to return the equilibrium value ($\eta_{eq} \equiv 1$), without making oscillation about η_{eq} . This behavior is typical of the overdamped regime.

As anticipated in Section 4.1.1, we would like to evaluate the reflectivity of the system in the region where the laser effects are high. To obtain this, we make an average of the order parameter along a line, starting at $(r = 0$ m, $z = 0$ m) and finishing at $(r = 0$ m, $z = w)$.

In the particular case of the current section, where the thickness d of the cylinder is longer than l_{pen} , we choose $w = l_{pen}$.

As for $|\langle \delta\eta \rangle|$, all the considerations expressed in Section 4.1.1 holds.

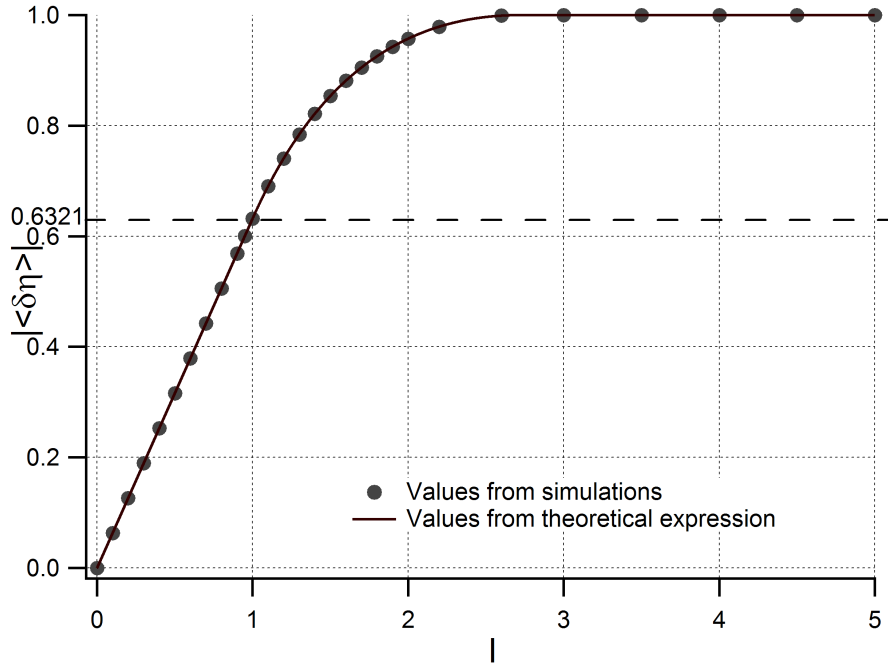


Figure 4.20: Plot of $|\langle \delta\eta \rangle|$ as a function of the laser intensity I , for the initial time $t = 0$ s and $l_{pen} = 0.03$ m. Here we report the values obtained from the simulations (markers) and the values obtained with the theoretical expression (continuous line).

As you can see from last picture, the values from simulations follow very well the theoretical equation, calculated for $w = l_{pen} = 0.03$ m. When the intensity grows from 0 to 1, $|\langle \delta\eta \rangle|$ increases proportionally, as predicted by equation (4.7). The theoretical coefficient of proportionality is 0.632121.

As time passes, the order parameter tends to return to the equilibrium value. So the values of $|\langle \delta\eta \rangle|$ diminish with time. The more intensity used, the more the system is perturbed, the more time is necessary to return to the equilibrium value (see figure 4.21).

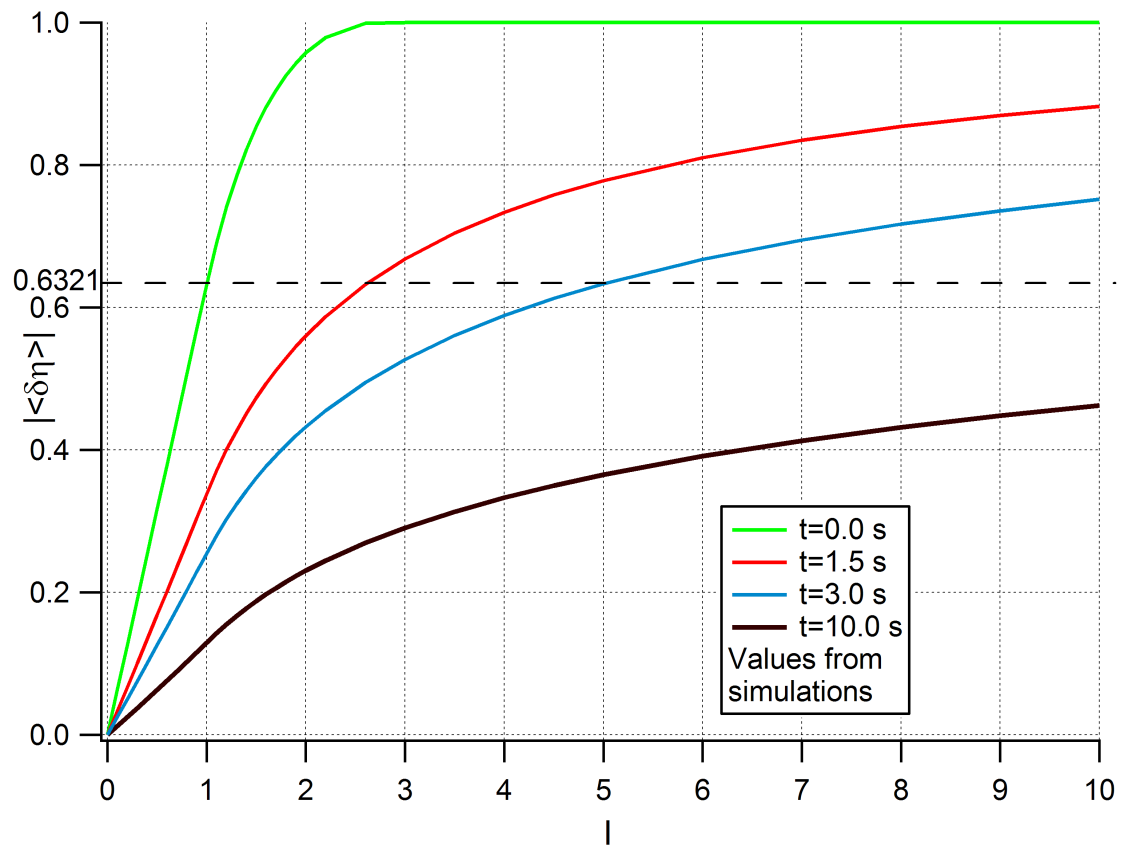


Figure 4.21: Plot of $|\langle \delta\eta \rangle|$ as a function of the laser intensity I , for different times and $l_{pen} = 0.03$ m. These results are obtained from simulations.

4.1.5 Comparison of the analyzed cases

In the following figure we plot $|\langle \delta\eta \rangle|$ as a function of I at the initial time, for all the cases of l_{pen} analyzed:

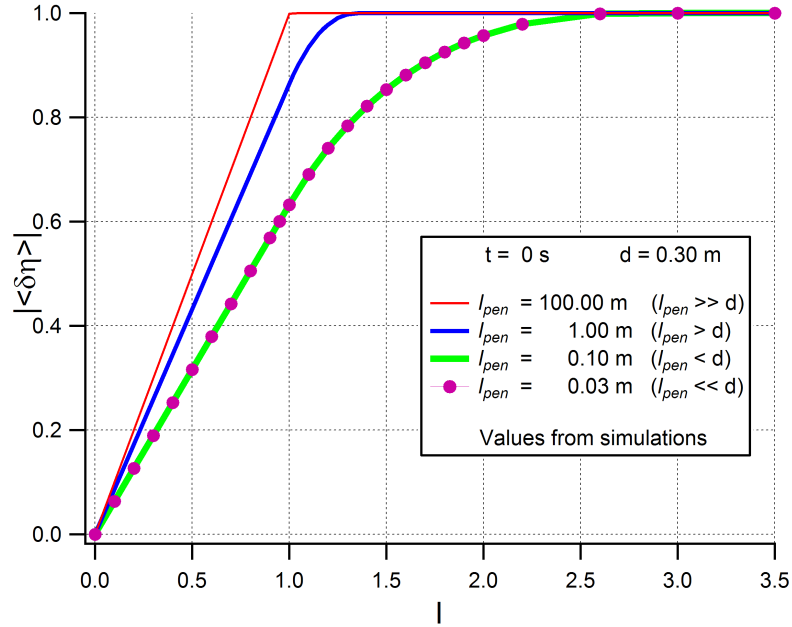


Figure 4.22: Plot of $|\langle \delta\eta \rangle|$ as a function of the laser intensity I , for different values of l_{pen} , for thickness $d = 0.3$ m and for $t = 0$ s. These results are obtained from simulations.

At $t = 0$ s, when $I = 1$, for $l_{pen} \gg d$ the system is saturated over the average line. Increasing the intensity $|\langle \delta\eta \rangle|$ does not change.

As l_{pen} decreases, the laser penetrates less, therefore the threshold moves to higher values of intensity.

Finally, at the initial time we obtain the same graph for the cases $l_{pen} = 0.1$ m and $l_{pen} = 0.03$ m. This agrees with the theoretical expressions (4.7) - (4.9), showing that if $w = l_{pen}$, then $|\langle \delta\eta \rangle|$ does not depend on l_{pen} .

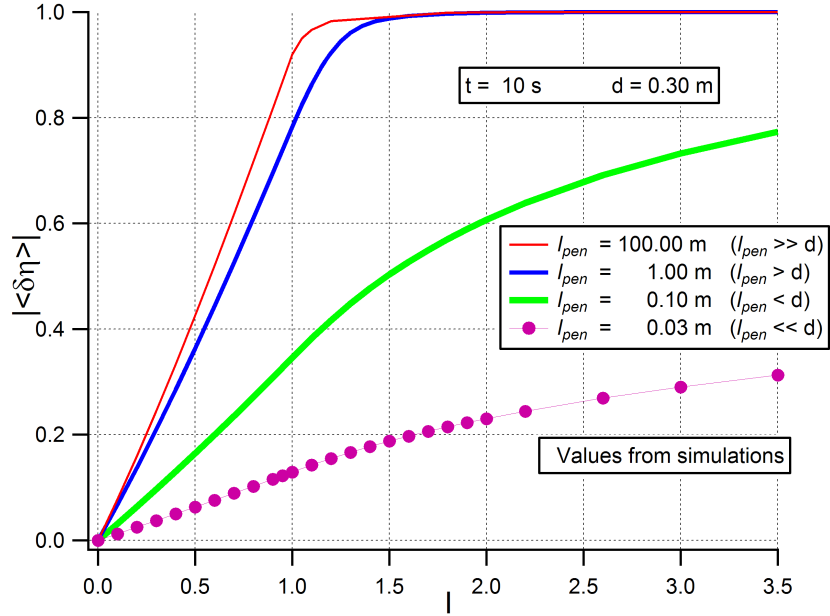


Figure 4.23: Plot of $|\langle \delta\eta \rangle|$ as a function of the laser intensity I , for different values of l_{pen} , for thickness $d = 0.3\text{ m}$ and for $t = 10\text{ s}$. These results are obtained from simulations.

After 10 s, for each intensity I , $|\langle \delta\eta \rangle|$ decreases with l_{pen} . Actually if l_{pen} is large, the perturbation is more significant and it is necessary more time to restore the equilibrium value.

4.1.6 Bulk system: comparison between simulations and experimental data

In this section the experimental data for the reflectivity will be compared with the simulations, using relation (4.3).

Since the experiments have been performed on a sample with a thickness larger than the penetration length of the light, it is necessary to compare the experimental outcomes to the simulations for a bulk system (case analyzed in section 4.1.4).

First of all we would like to find the temporal scale τ at which the order parameter has restored to his equilibrium value. Therefore for some values of laser intensity I we fit $|\langle \delta\eta \rangle|$, as a function of time, with a decreasing exponential:

$$y_0 + H_0 \exp\left(-\frac{t}{\tau_{fit}}\right).$$

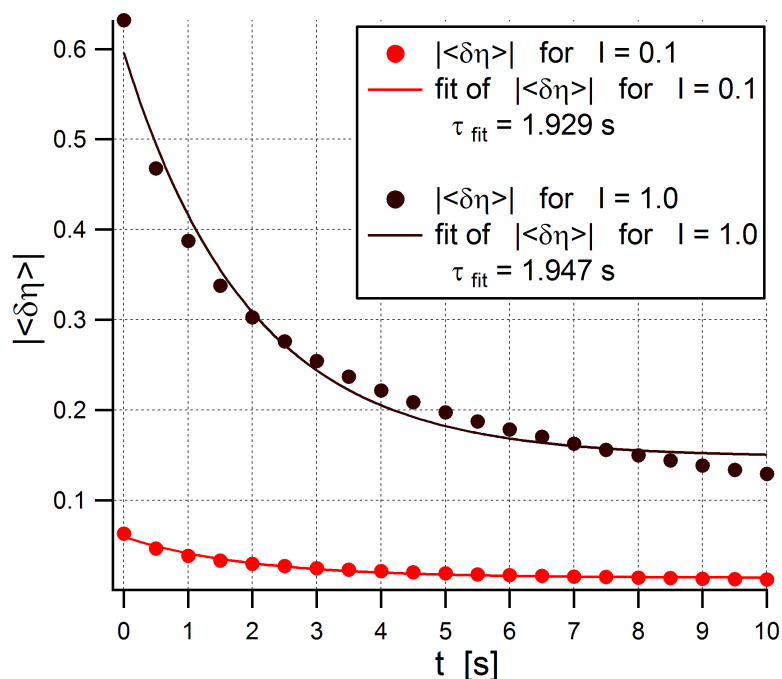


Figure 4.24: Markers: plot of $|\langle \delta\eta \rangle|$ as a function of time for $I = 0.1$ and $I = 1.0$, for $l_{pen} = 0.03$ m. Continuous line: fit with a decreasing exponential. These results are obtained from simulations.

Therefore we obtain $\tau_{fit} \sim 2$ s for any analyzed intensity.

However, for $I > 1$ the value of $|\langle \delta\eta \rangle|$ at the initial time has been introduced as a piecewise function, so the evolution in time of $|\langle \delta\eta \rangle|$ does not follow an exponential function (see figure 4.25) and so it does not make sense to look for a τ_{fit} in the high intensity simulations.

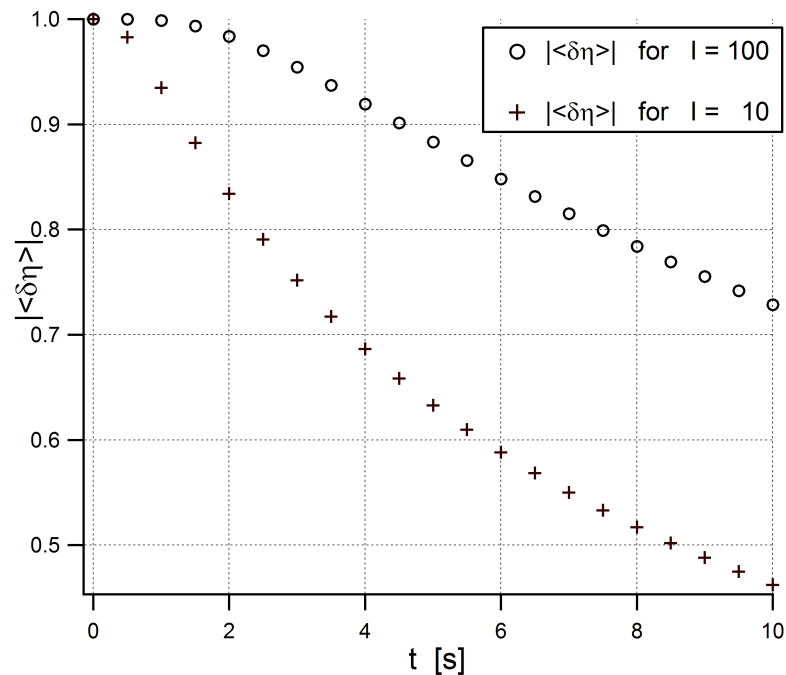


Figure 4.25: Plot of $|\langle \delta\eta \rangle|$, as a function of time, for $I = 10$ and $I = 100$, for $l_{pen} = 0.03$ m (data from simulations).

Experimental data¹ refer to a 30 K superconductor sample of $\text{Bi}_2\text{Sr}_2\text{Ca}_{0.92}\text{Y}_{0.08}\text{Cu}_2\text{O}_{8+\delta}$, hit by laser pulses (at repetition rate of 250 kHz), with a power up to 8 mW, a pulse width of 150 fs and wavelength centered at 800 nm. The laser spot size (spot diameter) is $80 \mu\text{m}$ ($\pm 10 \%$).

In the experiment the laser pulse hits the sample and then, as time passes, the reflectivity is measured.

¹Data taken from: G. Coslovich, C. Giannetti, F. Cilento, S. Dal Conte, G. Ferrini, P. Galinetto, M. Greven, H. Eisaki, M. Raichle, R. Liang, A. Damascelli, F. Parmigiani, *Evidence for a photoinduced nonthermal superconducting-to-normal-state phase transition in overdoped $\text{Bi}_2\text{Sr}_2\text{Ca}_{0.92}\text{Y}_{0.08}\text{Cu}_2\text{O}_{8+\delta}$* , PHYSICAL REVIEW B 83, 064519 (2011).

Using a polarizer, the intensity of the laser has been changed. Therefore it is possible to see the behavior of the reflectivity as time passes, for different values of impinging laser intensity.

We call I_N the normalized laser intensity ($I_N = I_N^{max} = 1$ is when all the power of the laser pulse passes through the polarizer).

As we did for the simulations, we would like to find the temporal scale τ_{fit} at which the order parameter has restored to his equilibrium value. Therefore for some values of I_N we fit the reflectivity (R) values, as a function of time, with a decreasing exponential:

$$y_0 + H_0 \exp \left[-\frac{(t - \hat{t}_0)}{\tau_{fit}} \right].$$

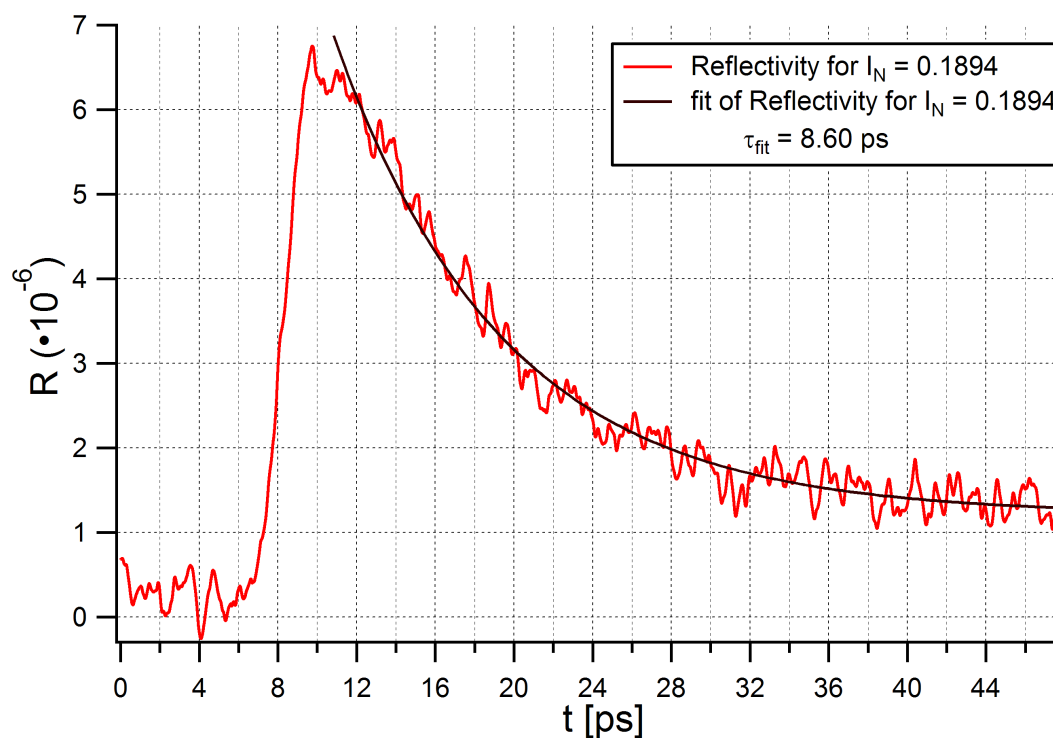


Figure 4.26: Plot of R , as a function of time, for $I_N = 0.1894$ (data from experiment).

For all the analyzed laser intensities we obtained $\tau_{fit} \sim 8$ ps.

Now we would like to analyze the system at short times after the laser pulse, i.e. where the effect of the perturbation is large.

- We choose to analyze the reflectivity of the system, as a function of the laser intensity, after 25 % of τ_{fit} (i.e. after 2 ps, for the analyzed case) from the laser pulse switching off.
- For each studied I_N we average the reflectivity from 13.30 ps to 13.31 ps, because the laser switching off was at the moment $\hat{t}_0 \sim 11$ ps on the used temporal scale (see figure 4.26).
- We note that the average over a short time interval (100 fs) could be affected by noise. To avoid this problem, we make also a second analysis, averaging on a larger time interval: for each studied I_N we average the reflectivity from 10 ps to 13 ps.
- We normalize the value of reflectivity, dividing it by its maximum value. So we obtain the normalized average reflectivity $\langle R \rangle$, see markers in figure 4.27.
- We would like to compare the experimental $\langle R \rangle$ with $|\langle \delta\eta \rangle|$ from simulations. Therefore we analyze $|\langle \delta\eta \rangle|$ after 0.5 s (25 % of τ_{fit}), see blue line in figure 4.27.

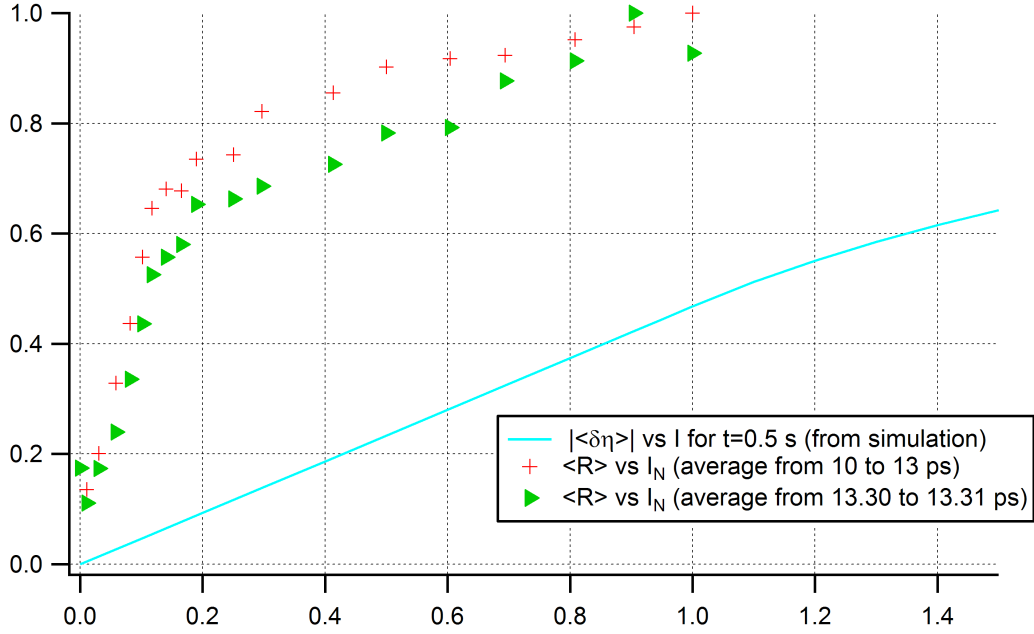


Figure 4.27: Blue continuous line: plot of $|\langle \delta\eta \rangle|$ as a function of the laser intensity I for $t = 0.5$ s (values from simulations). Red markers: plot of $\langle R \rangle$ as a function of the normalized laser intensity I_N (average made from 10 ps to 13 ps). Green markers: plot of $\langle R \rangle$ as a function of the normalized laser intensity I_N (average made from 13.30 ps to 13.31 ps).

From this figure we note that in both cases $\langle R \rangle$ has the same functional behavior of $|\langle \delta\eta \rangle|$. However $\langle R \rangle$ reaches the saturation for $I_N = 1$, while $|\langle \delta\eta \rangle|$ saturates for $I = 250$.

Actually I and I_N have not the same meaning, because we do not know which physical situation correspond to a certain I_N . Therefore we would like to find the relation between I and I_N .

$I_N = 1$ means that the sample is excited by the maximum laser intensity available from the used experimental setup. Evidently a region of the sample has been brought in the state with $\eta = 0$.

Comparing $\langle R \rangle$ graph and $|\langle \delta\eta \rangle|$ graph², we would like to define the region

²We assume that relation (4.3) holds. Since we are dealing with a normalized reflectivity, we can deduce $\gamma = 1$ in this case.

of the experimental system in which the order parameter is brought to 0. In other words when we choose a certain laser intensity I_N in the experiments we generate a certain physical situation. We would like to find the value of I (in the simulations) which generates the solution of GL equation reproducing that physical situation.

1. We want to have $|\langle \delta\eta \rangle|$, as a function of I , evaluated in $2 \cdot 10^6$ values of I ranging from $I = 0$ to $I = 10^3$.

To obtain $|\langle \delta\eta \rangle|$ for one value of I we have to make one simulation. Instead of making $2 \cdot 10^6$ simulations (very expensive and time wasting procedure), we run a few simulations (for a few values of I), so that we can see the behavior of $|\langle \delta\eta \rangle|$, as a function of I , for the desired interval from $I = 0$ to $I = 10^3$. Then we use COMSOL Multiphysics to make an interpolation of this function, to obtain all the $2 \cdot 10^6$ values of $|\langle \delta\eta \rangle|$.

2. Using MATLAB software we tune the parameter ε from 0 to 201, with a step of 1.
3. For each value of I_N , we search the value (which is labeled with $I_{near}^{[I_N]}$) of interpolated intensity nearest to $\varepsilon \cdot I_N$. Then we evaluate:

$$f_{ms}(\varepsilon) = \sum_{I_N} \{ |\langle \delta\eta (I_{near}^{[I_N]}) \rangle| - \langle R(\varepsilon \cdot I_N) \rangle \}^2.$$

We make this step for all the tuned values of ε .

4. We look for the ε at which $f_{ms}(\varepsilon)$ assumes the minimum value.
5. We repeat the last 2 steps, with ε tuned around the minimum (with a step of 0.01). So we find a more precise minimum (ε_{min}).

We execute this algorithm for the two sets of $\langle R \rangle$ (reported in figure 4.27) and we obtain the ε_{min} values reported in the following table:

	Average from 13.30 ps to 13.31 ps	Average from 10 ps to 13 ps
Symbol in Graphics	▶	+
ε_{min}	6.43	11.12
Threshold Fluence [$\frac{\mu\text{J}}{\text{cm}^2}$]	99.0 (± 20 %)	57.2 (± 20 %)

Using the conversion

$$I = \varepsilon_{min} I_N, \quad (4.10)$$

the experimental data can be compared directly with simulations.

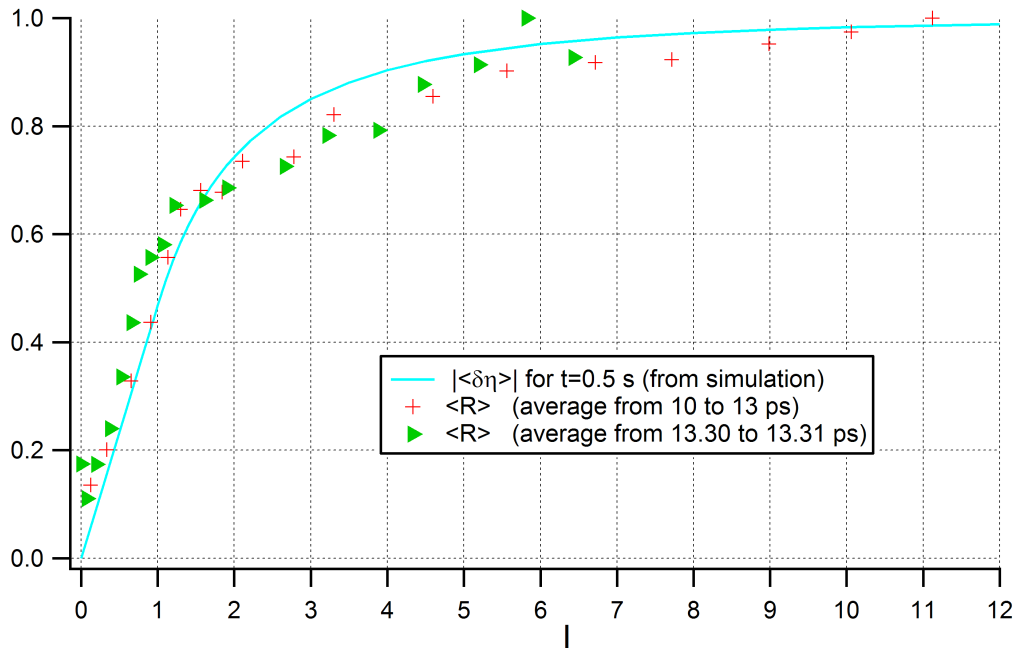


Figure 4.28: Blue continuous line: plot of $|\langle \delta\eta \rangle|$ as a function of the laser intensity I for $t = 0.5$ s (values from simulations). Red markers: plot of $\langle R \rangle$ as a function of the intensity $I = 11.12 \cdot I_N$ (average made from 10 ps to 13 ps). Green markers: plot of $\langle R \rangle$ as a function of the intensity $I = 6.43 \cdot I_N$ (average made from 13.30 ps to 13.31 ps).

This figure shows that both the sets of $\langle R \rangle$ data have a behavior similar to $|\langle \delta\eta \rangle|$. However, the set obtained as a long time average (red marker in figure 4.28) follows $|\langle \delta\eta \rangle|$ better: using a short time average we see the effects of the noise.

It is important to point out that $I = 1$ in simulations is the threshold value at which you begin to have $\eta = 0$ in one point in the system - i.e. the broken symmetry has been restored in that point.

In the case of a superconductor, for instance, the system is brought in normal state in the region where $\eta = 0$.

Therefore, from the conversion relation (4.10), we can say that the threshold laser intensity is $I_N^{th} = 1/\varepsilon_{min}$.

Reminding that I_N is normalized, we have the following relation:

$$\frac{I_N^{th}}{I_N^{max}} = I_N^{th} = \frac{1}{\varepsilon_{min}}.$$

So the power to apply in order to have the threshold situation is:

$$\begin{aligned} \text{Threshold Power} &= \frac{\text{Threshold Power}}{\text{Maximum Power}} \cdot \text{Maximum Power} = \\ &= \frac{I_N^{th}}{I_N^{max}} \cdot \text{Maximum Power} = \frac{1}{\varepsilon_{min}} \cdot \text{Maximum Power} = \frac{1}{\varepsilon_{min}} \cdot 8 \text{ mW} \end{aligned}$$

and therefore the energy per pulse to have the threshold situation is:

$$\frac{1}{\varepsilon_{min}} \cdot \frac{\text{Maximum Power}}{\text{Repetition Rate}} = \frac{1}{\varepsilon_{min}} \cdot \frac{8 \text{ mW}}{250 \text{ kHz}}.$$

Finally we can introduce the fluence to have the threshold situation as the corresponding energy per pulse divided by the laser spot area:

$$\begin{aligned} \text{Threshold Fluence} &= \frac{1}{\varepsilon_{min}} \cdot \frac{\text{Maximum Power}}{\pi \left(\frac{\text{Spot Diameter}}{2}\right)^2 \cdot \text{Repetition Rate}} = \\ &= \frac{1}{\varepsilon_{min}} \cdot \frac{8 \text{ mW}}{\pi \left(\frac{80 \mu\text{m}}{2}\right)^2 \cdot 250 \text{ kHz}}. \end{aligned}$$

The obtained threshold fluence values are reported in the last table.

The error for the threshold fluence is due to the propagation of the spot diameter error.

The obtained threshold fluence values can be compared with the experimental one (Φ_C), estimated as the value at which there is the transition from a low excitation regime (when the fluence is small and $\langle R \rangle$ increases proportionally to the fluence) to a high excitation regime (when the fluence is high and $\langle R \rangle$ has a sub-linear dependence on the fluence).

The threshold fluence values obtained from simulations have the same order of magnitude of the experimental fluence (estimated as $\Phi_C = 26 \mu\text{J}/\text{cm}^2$). However due to the big error on the spot diameter, the values obtained from simulations are not very precise.

4.2 Technical details

To obtain the data in Chapter 4 we use a “2D-Axisymmetric Model”, with a “Coefficient Form PDE” physics.

Then we introduce the model parameters. Since in COMSOL Multiphysics we cannot use Greek letters as parameters, we use:

Parameter names in COMSOL Multiphysics	Corresponding parameter in our work
<i>omega</i>	ω
<i>alpha</i>	α
<i>lambda</i>	λ
<i>A</i>	<i>A</i>
<i>B</i>	<i>B</i>
<i>penetrazione</i>	l_{pen}
<i>larghezza</i>	l_{width}
<i>I</i>	<i>I</i>

The parameters used for each simulation are specified near the reported results.

Geometry:

- The geometry used is a rectangle 2 m \times 0.3 m, built in the (r, z) plain (with reference to figure 4.7).

If $I > 1$, the geometry is more complicate:

- We create a parametric curve to define the parabola introduced in equation (4.4). The dimensionless parameter s , defining the parametric curve, has to represent the variable r in equation (4.4). So we assign the following expression to r coordinate in the “Expressions” field:

$$s * 1 \text{ [m]}.$$

To obtain the parabola, the parameter s ranges from 0 to

$$larghezza * sqrt(log(I))/1 \text{ [m]}.$$

In COMSOL Multiphysics “*log*” stands for natural logarithm and “*sqrt*” stands for square root.

Then we write the following expression for z coordinate in the “Expressions” field:

$$(-s^2 * 1 \text{ [m}^2\text{]}/larghezza^2 + \log(I)) * penetrazione.$$

So we obtain a parabola.

Finally, in “Position” field we set $r = 0$ and $z = 0$. We write 0 in the “Rotation Angle” field.

- We create a segment:
from $(r = 0, z = 0)$ to $(r = larghezza * \sqrt{\log(I)}, z = 0)$
and a segment:
 $(r = 0, z = 0)$ to $(r = 0, z = \log(I) * penetrazione)$.

To create a segment we right-click over the voice “Geometry” and we choose “Bézier Poligon”. Then we choose “Open curve” in the “Type” field, and click on “Add linear”. So we can introduce the coordinates of the segment beginning and end.

- We right-click on “Geometry”, we choose “Boolean operation \rightarrow Union”, we select the parabola and the 2 segments to make the union (we select “Keep interior boundaries”).
The “Union” of the parabola and the 2 segments generates a closed curve.
- We right-click on “Geometry”, we choose “Conversions \rightarrow Convert to Solid”, we select the closed curve obtained from the “Union” in the last step, to make an irregular plane figure, surrounded by that closed curve.
- We right-click on “Geometry”, we choose “Boolean operation \rightarrow Difference”, we select the rectangle as “Object to add” and the irregular plane figure generated in the last step as “Object to subtract” to create the “domain 2” (we select “Keep interior boundaries” and “Keep input objects”).
- We right-click on “Geometry”, we choose “Boolean operation \rightarrow Intersection”, we select the rectangle and the irregular plane figure generated in the previous steps to create the “domain 1” (we select “Keep interior boundaries”).
“domain 1” and “domain 2” are drawn in figure 4.29.
- If $penetrazione < 0.3 \text{ m}$ we create a segment:
from $(r = 0, z = 0)$ to $(r = 0, z = penetrazione)$,
over which the solution will be averaged. If $penetrazione < 0.3 \text{ m}$, we do

not need to create this segment, because the average will be made on the boundary of the rectangle.

Clicking on “Coefficient Form PDE” we choose “Dimensionless” as “Dependent variable quantity” (u), “None” for the “Source term quantity” field and 1 for the “Unit” field.

Then we introduce the coefficient in the “Coefficient Form PDE”; referring to equation (2.1):

$$e_a \frac{\partial^2 u}{\partial t^2} + d_a \frac{\partial u}{\partial t} + \nabla \cdot (-c \nabla u - \boldsymbol{\alpha} u + \boldsymbol{\gamma}) + \boldsymbol{\beta} \cdot \nabla u + a u = f, \quad (2.1)$$

we assign the following coefficients:

Terms in equation (2.1)	Assigned coefficients
c	$lambda$ (Isotropic)
a	A
f	$-B * u^3$
e_a	$1/omega^2$
d_a	$alpha/omega$
$\boldsymbol{\alpha}$	$(0, 0)$
$\boldsymbol{\beta}$	$(0, 0)$
$\boldsymbol{\gamma}$	$(0, 0)$

As boundary conditions we apply “Zero Flux” boundary condition to all external boundaries (see next figure).

COMSOL Multiphysics applies automatically continuity of the solution u and of $c \nabla u$ at the internal boundaries, since we do not assign them an explicit condition.

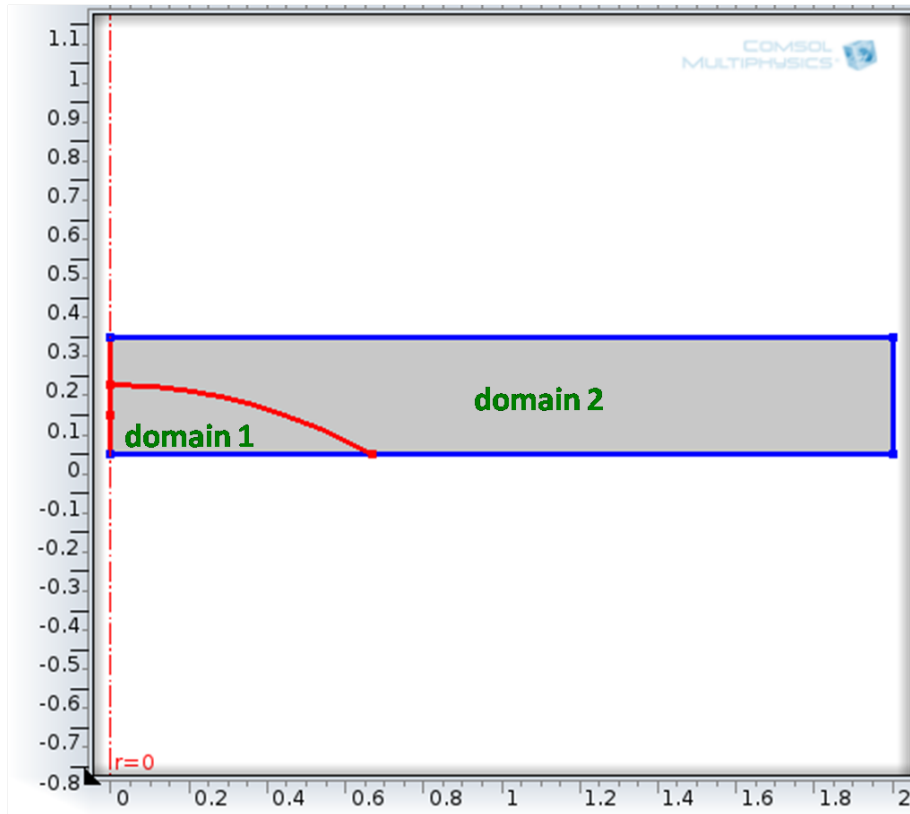


Figure 4.29: Plot of the geometry of the system, in the case of $l_{pen} = 0.1$ m and $I = 6$. We apply “Zero Flux” boundary condition to the blue lines. The program applies automatically continuity of u and of $c\nabla u$ at the red lines.

As per the “Initial values”:

- In the case $I \leq 1$ we type:

$$1 - I * \exp(-z/penetrazione) * \exp(-r^2/larghezza^2)$$

at the voice “Initial value for u”, and 0 at the voice “Initial time derivative of u”, applied to the unique domain.

- In the case $I > 1$ we right-click on “Coefficient Form PDE” voice and add an “Initial values” node.

At the “domain 1”, we type 0 at the voice “Initial value for u”, and 0 at the voice “Initial time derivative of u”.

At the “domain 2”, we type

$$1 - I * \exp(-z/penetrazione) * \exp(-r^2/larghezza^2)$$

at the voice “Initial value for u”, and 0 at the voice “Initial time derivative of u”.

As per the Mesh we choose a “Physics-controlled mesh”, with “Extremely fine” element size (that is to say a triangular Mesh with 0.02 m as “Maximum element size”).

We use a “Time Dependent Study”, with “Generalized alpha” time stepping method. The steps taken by solver are manual, with a time step of 10^{-2} .

When the numerical solution is obtained we make an average, right clicking on “Derived Values” node and choosing “Average → Line Average”. Then under the voice “Line Average” we select the domains over which we want to average.

References

1. G. Coslovich, C. Giannetti, F. Cilento, S. Dal Conte, G. Ferrini, P. Galinetto, M. Greven, H. Eisaki, M. Raichle, R. Liang, A. Damascelli, F. Parmigiani, *Evidence for a photoinduced nonthermal superconducting-to-normal-state phase transition in overdoped $\text{Bi}_2\text{Sr}_2\text{Ca}_{0.92}\text{Y}_{0.08}\text{Cu}_2\text{O}_{8+\delta}$* , PHYSICAL REVIEW B 83, 064519 (2011).
2. Claudio Giannetti, Giacomo Coslovich, Federico Cilento, Gabriele Ferrini, Hiroshi Eisaki, Nobuhisa Kaneko, Martin Greven, Fulvio Parmigiani, *Discontinuity of the ultrafast electronic response of underdoped superconducting $\text{Bi}_2\text{Sr}_2\text{CaCu}_2\text{O}_{8+\delta}$ strongly excited by ultrashort light pulses*, PHYSICAL REVIEW B 79, 224502 (2009).
3. Claudio Giannetti, Federico Cilento, Sstefano Dal Conte, Giacomo Coslovich, Gabriele Ferrini, Hajo Mmolegraaf, Mmarkus Raichle, Ruixing Liang, Hiroshi Eisaki, Mmartin Greven, Andrea Damascelli, Dirk van der Mmarel, Fulvio Parmigiani, *Revealing the high-energy electronic excitations underlying the onset of high-temperature superconductivity in cuprates*, Nature Communications (2011).

Chapter 5

Super-lattice composed by materials with broken symmetry

In this brief chapter we would like to expose some possible applications of our work.

It is worth to introduce a super-lattice, characterized by a periodic unit cell composed by layers of different materials. In our analysis, the chosen materials support a real order parameter, satisfying GL equation (1.13).

Therefore this theory applies to all materials with a broken symmetry, in particular superconductors or ferromagnetic materials.

We would like to analyze how a perturbation of the order parameter propagates through the super-lattice. For this purpose we choose materials with low damping ($\alpha \ll 1$). Therefore GL equation reduces to:

$$\frac{1}{\omega^2} \frac{\partial^2 \eta}{\partial t^2} - \lambda \nabla^2 \eta + A(P, T) \eta + B(P) \eta^3 = 0. \quad (5.1)$$

Equation (5.1) has the form of a wave equation (the first 2 terms) with a source term (the last 2 terms).

For sake of simplicity, we work with a 1D super-lattice, with a unit cell characterized by 2 layers of different material.

The general solution of equation (5.1) can be written using the Fourier transform:

$$\eta(x, t) = \int_{-\infty}^{+\infty} \int_{-\infty}^{+\infty} \tilde{\eta}(k, \omega) e^{ikx} e^{i\omega t} dk d\omega.$$

Considering that the equation (5.1) should be solved for the super-lattice geometry, ω must be related to k by a *dispersion relation*:

$$\omega = f(k).$$

Our target is to work out the dispersion relation, very useful to predict how a wave packet propagates through the super-lattice.

The dispersion relation can predict if a certain frequency cannot pass through the super-lattice, if there are no k values allowed for that frequency. The dispersion relation can show if there are *frequency gaps*, i.e. zones in the frequency spectrum whose frequencies does not pass through the super-lattice.

The dispersion relation can predict the velocity of propagation of a certain frequency in the super-lattice.

Actually the dispersion relation should depend on the choice of the materials and on the geometry of the built unit cell. With an opportune choice of the materials composing the super-lattice or of the unit cell geometry, we can modify the dispersion relation.

A possible application is the creation of a frequencies filter: with an opportune choice of the materials we can control the frequency gaps of the super-lattice so that only certain desired frequencies in a wave packet can pass through the super-lattice.

There are different possibilities to simulate this physical situation. In our work we treat:

1. A “many unit cells geometry”: the super-lattice is approximated by repeating a lot of times the unit cell. So we see the behavior of a finite super-lattice, but if we repeat the unit cell for a high number of times the final solution will be a good approximation to the theoretical infinite super-lattice.
2. A “one unit cell geometry”: we analyze the behavior of a single unit cell. To reproduce the infinite super-lattice behavior we apply a periodic boundary condition.

5.1 Many unit cells geometry

We build a super-lattice composed by 6 unit cells. Each unit cell is composed by two layers of two different materials (called “Material 1” and “Material 2”). We suppose that the two used materials satisfy the GL equation (5.1), and that they have the same coefficients ω , λ , B , but A coefficient can be different. The super-lattice is put between 2 slices, an initial layer and a detector layer, made of “Material 1”, see figure 5.1.



Figure 5.1: The super-lattice. The black segments represent the “Material 1”, the orange segments represent the “Material 2”. The used system of coordinate is indicated.

In this section we would like to see how a wave packet propagates through the super-lattice. This wave packet is produced by perturbing the order parameter with a laser pulse (switching off at time $t = 0$ s), at the beginning of the system ($x = 0$).

Since we want to analyze how the pulse passes through the super-lattice, we impose zero-flux boundary condition at the external boundaries, so the system is isolated from the external world and we are sure that all the perturbation is driven towards the super-lattice. From one layer to another we impose the continuity of the solution and of the first spatial derivative of the solution.

We use COMSOL Multiphysics to obtain a numerical solution of equation (5.1). First we seek the equilibrium solution η_{eq} solving equation (5.1) with a “stationary study”.

Next we would like to solve the equation (5.1) in the time domain. To simulate the laser pulse we choose the following expressions as initial values:

$$\eta(x, t = 0 \text{ s}) = \eta_{eq} [1 - I \exp(-x/l_{pen})], \quad (5.2)$$

$$\left. \frac{d\eta}{dt} \right|_{t=0} = 0 \text{ s}^{-1},$$

applied to all the domains.

Therefore at the initial time there is a wave packet before the super-lattice (decreasing exponential perturbation of the equilibrium order parameter). This packet will evolve and we would like to see if the perturbation passes the super-lattice.

We compute simulations keeping fixed the following parameters:

- $\omega = 0.1 \text{ s}^{-1}$;
- $\lambda = 0.18 \text{ m}^2$;
- $l_{pen} = 1 \text{ m}$;
- $B = 1$ (dimensionless).

In “Material 1” we fix $A = -1$, while in “Material 2” we use different values of A (for simplicity we use the notation A_2 to mean the coefficient A used in the “Material 2”), so that we can have a low or a high contrast between the two materials.

As for the geometry, we choose a unit cell composed by a 4 m layer of “Material 2” and a 4 m layer of “Material 1”. Then we use a 4 m initial layer and a 20 m detector layer.

We make a simulation with $A_2 = -0.9$, i.e. the difference between the two materials is little. The results are exposed in figure 5.2, in which you can see the order parameter behavior (color scale) in the super-lattice geometry (horizontal axis) and in time (vertical axis).

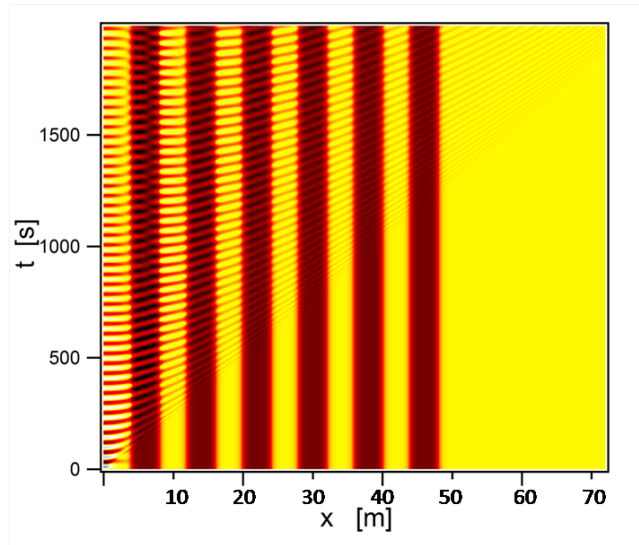


Figure 5.2: The evolution of the order parameter (color scale) in the geometry, as a function of time, for $A_2 = -0.9$.

Then we make another simulation in which $A_2 = -0.1$, i.e. the difference between the 2 materials is important. The results are exposed in figure 5.3,

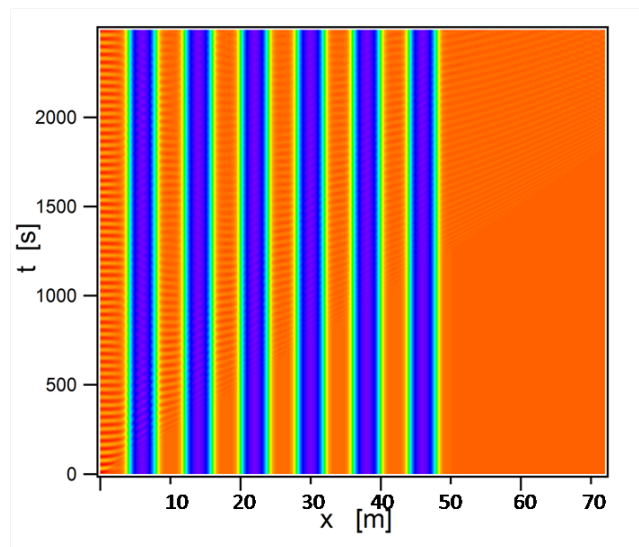


Figure 5.3: The evolution of the order parameter (color scale) in the geometry, as a function of time, for $A_2 = -0.1$.

As you can see, in the initial layer the order parameter oscillates in time, in agreement with the fact that we are dealing with an undamped system.

You can also see that the order parameter passes through the super-lattice, arriving in the detector layer. However in the detector layer the perturbation intensity is lower, because the wave packet spreads during the travel through the super-lattice.

5.2 One unit cell geometry

We can build a unit cell composed by two different materials (called “Material 1” and “Material 2”).

We suppose that the two used materials satisfy the GL equation (5.1), and that they have the same coefficients ω , λ , B , but A coefficient can be different.

We work with a unit cell of length d , characterized by the geometry shown in figure 5.4. As you can see half of the unit cell is made of “Material 1” and half of “Material 2”.

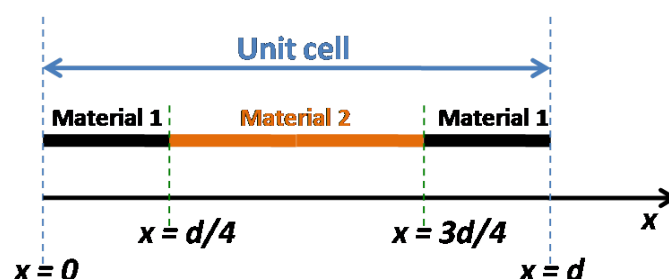


Figure 5.4: The unit cell. The black segments represent the “Material 1”, the orange segment represents the “Material 2”.

Assuming that the order parameter is slightly perturbed from the equilibrium value (i.e. $\delta\eta(x, t) = \eta(x, t) - \eta_{eq}(x)$ is small) we can assume that the linearized GL equation (introduced in section 1.4):

$$\frac{1}{\omega^2} \frac{\partial^2 \delta\eta}{\partial t^2} - \lambda \frac{\partial^2 \delta\eta}{\partial x^2} + [A + 3B(\eta_{eq})^2] \delta\eta = 0, \quad (5.3)$$

holds in all the unit cell.

Then we would like to simulate the periodicity of the unit cell, so we assume that the order parameter satisfies the Bloch condition:

$$\delta\eta(x, t) = e^{ikx} u_k(x, t), \quad (5.4)$$

with $u_k(x = 0, t) = u_k(x = d, t)$.

In the current section we focus our attention at the center of the first Brillouin zone, therefore we fix $k = 0 \text{ m}^{-1}$.

Therefore we make the substitution $\delta\eta(x, t) = u_0(x, t)$ in equation (5.3) to obtain:

$$\frac{1}{\omega^2} \frac{\partial^2 u_0}{\partial t^2} - \lambda \frac{\partial^2 u_0}{\partial x^2} + [A + 3B (\eta_{eq})^2] u_0 = 0. \quad (5.5)$$

For both materials we choose the following parameters:

- $\omega = 0.1 \text{ s}^{-1}$;
- $\lambda = 0.18 \text{ m}^2$;
- $B = 1$ (dimensionless).

In “Material 1” we fix $A = -1$.

For simplicity we use the notation A_2 to mean the coefficient A used in the “Material 2”. We make some simulations changing the value of A_2 (i.e. changing the contrast between the 2 used materials).

As for the geometry, we choose a unit cell with length $d = 8 \text{ m}$.

For each value of A_2 , we make a simulation using COMSOL Multiphysics. In particular we solve the equilibrium equation (1.10) for a real order parameter numerically, with a “Stationary Study”, to evaluate η_{eq} ; then we use the equilibrium value found to look for the first 10 eigenvalues of equation (5.5).

In figure 5.5 we report the relative distance between the second and the third eigenvalue ($\Delta\omega_{eig}$), as a function of the value of A_2 coefficient.

As you can see, when the unit cell is composed by an homogeneous material ($A_2 = -1$) the second and the third eigenvalue are degenerate.

When A_2 increases, the contrast between the 2 used materials grows. The second and the third eigenvalue split and so we can understand that there is a gap in the frequency spectrum. The more the “Material 2” is different from the “Material 1” (the more A_2 grows in our simulations), the more the frequency gap increases.

It is also interesting to point out that the gap value is appreciable, because it is up to 15% of the eigenvalue values.

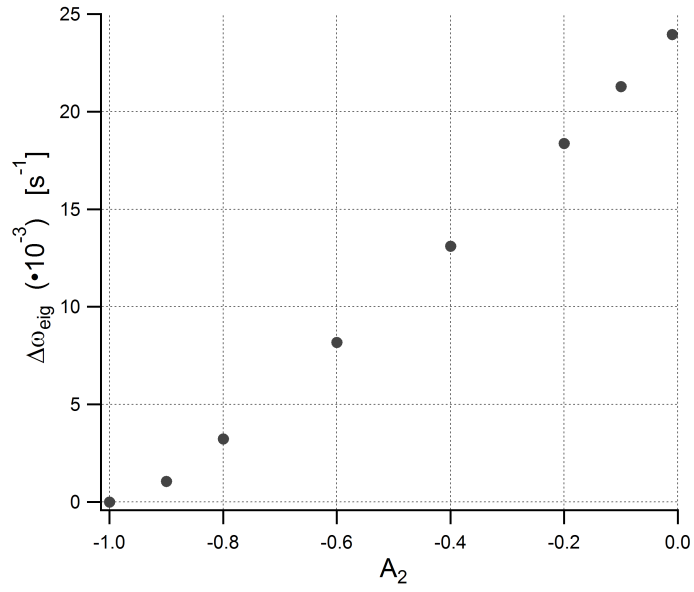


Figure 5.5: Plot of $\Delta\omega_{eig}$ vs A_2 . Reminding that in “Material 1” we use $A = -1$, the contrast is high when A_2 is near to 0.

Appendix

Remarks about the damped harmonic oscillator

In this section we report the solutions of the damped harmonic oscillator differential equation.

A damped harmonic oscillator satisfies the differential equation:

$$\frac{\partial^2 x}{\partial t^2} + \alpha\omega \frac{\partial x}{\partial t} + \omega^2 x = 0, \quad (1)$$

with $\alpha > 0$ and $\omega > 0$.

To solve it we look for the solutions of the following equation:

$$\lambda^2 + \alpha\omega\lambda + \omega^2 = 0. \quad (2)$$

We have 3 possibilities:

1. *Underdamped harmonic oscillator*, if

$$\Delta = \alpha^2\omega^2 - 4\omega^2 < 0, \quad (3)$$

(i.e. $\alpha < 2$).

In this case the solutions of (2) are:

$$\lambda_{\pm} = -\frac{\alpha\omega}{2} \pm i\sqrt{\frac{|\Delta|}{4}}.$$

Hence equation (1) has the general solution:

$$x(t) = \exp\left(-\frac{\alpha\omega}{2} t\right) \left[k_1 \exp\left(i\sqrt{\frac{|\Delta|}{4}} t\right) + k_2 \exp\left(-i\sqrt{\frac{|\Delta|}{4}} t\right) \right], \quad (4)$$

where k_1 and k_2 are constants which can be fixed using appropriate boundary conditions.

As you can see from solution (4), x oscillates with a decreasing in time amplitude.

2. *Overdamped harmonic oscillator*, if

$$\Delta = \alpha^2\omega^2 - 4\omega^2 > 0, \quad (5)$$

(i.e. $\alpha > 2$).

In this case the solutions of (2) are:

$$\lambda_{\pm} = -\frac{\alpha\omega}{2} \pm \sqrt{\frac{\Delta}{4}}.$$

Hence equation (1) has the general solution:

$$x(t) = k_1 \exp \left[\left(-\frac{\alpha\omega}{2} + \sqrt{\frac{\Delta}{4}} \right) t \right] + k_2 \exp \left[\left(-\frac{\alpha\omega}{2} - \sqrt{\frac{\Delta}{4}} \right) t \right], \quad (6)$$

where k_1 and k_2 are constants which can be fixed using appropriate boundary conditions.

From equation (5) we obtain:

$$\frac{\alpha\omega}{2} = \sqrt{\frac{\alpha^2\omega^2}{4}} > \sqrt{\frac{\alpha^2\omega^2}{4} - \omega^2} = \sqrt{\frac{\Delta}{4}},$$

which tells us that in equation (6) there are two decreasing exponential functions.

When α grows, the second exponential becomes smaller and the first exponential becomes larger. Therefore when α is large enough the first exponential dominates and $x(t)$ falls slowly to the equilibrium value with respect to the case of lower damping.

3. *Critically damped harmonic oscillator*, if

$$\Delta = \alpha^2\omega^2 - 4\omega^2 = 0, \quad (7)$$

(i.e. $\alpha = 2$).

In this case the solutions of (2) are degenerate:

$$\lambda_{\pm} = -\frac{\alpha\omega}{2}.$$

Hence equation (1) has the general solution:

$$x(t) = k_1 \exp\left(-\frac{\alpha\omega}{2} t\right) + k_2 t \exp\left(-\frac{\alpha\omega}{2} t\right), \quad (8)$$

where k_1 and k_2 are constants which can be fixed using appropriate boundary conditions.